THE UNIVERSITY OF MANITOBA

GRAIN BOUNDARIES AS DISLOCATION SOURCES

by

T. F. Malis

A THESIS

SUBMITTED TO THE FACULTY OF GRADUATE STUDIES

IN PARTIAL FULFILMENT OF THE REQUIREMENTS FOR THE DEGREE

OF DOCTOR OF PHILOSOPHY

DEPARTMENT OF MECHANICAL ENGINEERING

WINNIPEG, MANITOBA

January, 1975.

GRAIN BOUNDARIES AS DISLOCATION SOURCES

by

T. F. MALIS

A dissertation submitted to the Faculty of Graduate Studies of the University of Manitoba in partial fulfillment of the requirements of the degree of

DOCTOR OF PHILOSOPHY

ABSTRACT

GRAIN BOUNDARIES AS DISLOCATION SOURCES

By

T. F. Malis

An investigation was conducted into the role of grain boundaries as sources of lattice dislocations during yielding. An extensive review of the literature was conducted in order to establish a firm base for the study of this relatively new field. This included grain boundary structural models, the defect structure associated with the boundary, previous experimental confirmation of grain boundary source operation, and the proposed models for such sources, including the stress required and the means of enhancing the applied stress to this value.

An electron microscope examination was then conducted on several materials which possessed microstructures conducive to boundary sources and which had been strained to points well below and up to the yield point. Two techniques were developed to aid the thin foil examination. One led to a reduction in thin foil deformation due to foil handling, and the other was a thin foil mapping technique to provide comparative data on the densities and distributions of lattice defects pertinent to the

yield process.

The experimental results indicated that the great majority of boundary sources were nonregenerative in nature, and involved the nucleation and emission of both perfect and partial dislocations from grain boundary ledges. These dislocations were nucleated at low stresses and many were retained at the boundary. Emission occurred preferentially from triple points in the early stages of yielding. The proportion of strain contributed by boundary sources was negligible in high purity Al. In high purity Cu, the most extensively studied material, it was significant in only the first stage of what appeared to be a two-stage yielding process common to all the materials. In the second stage grain interior sources were predominant. In medium purity Ni, boundary sources were present in substantially larger numbers, and in Cu - 1 wt % Sn, they were present in sufficient numbers to control the major portion of the entire yield process. A number of factors, such as stacking fault energy or elastic anisotropy, appeared to influence boundary source characteristics or their operation, but the most important were the initial states of the boundaries and the distribution of solute or impurity atoms within the material.

With the experimental observations in mind, a detailed model of boundary sources was constructed. It

proposes dislocation nucleation from groups of small boundary ledges, with the ledge geometry providing the major portion of the necessary stress concentration for this nucleation. Additional stress concentration is supplied by interaction of the stress fields from the ledges within each group. The variation in the number, size and spacing of ledges within each group, along with the variation in individual ledge geometry, account for the observed non-homogeneous distribution of boundary sources. Several specific aspects of this model are then discussed, as well as its implications for other important facets of mechanical behavior.

ACKNOWLEDGMENTS

I would like to express my gratitude to the Steel Company of Canada Ltd., for their financial assistance. There are many people who rendered assistance during the course of this study, particularly Mr. J. Van Dorp, Dr. M. C. Chaturvedi, and Dr. D. J. Lloyd. I owe a special debt to my supervisor, Dr. K. Tangri. Through his teaching, criticism and encouragement, he has been instrumental in refining my capabilities as a scientist, with regards to both the conduction of research and the art of communicating it to others. Finally, I wish to thank my wife, Margaret, for her endurance of the student's life and the grueling pace often associated with completion of this work.

TABLE OF CONTENTS

Page

Page

LIST OF TABLES

LIST OF MICRO-MAPS

LIST OF FIGURES

Page

Page

Page

Page

1.0 INTRODUCTION

An overwhelming majority of engineering materials are used in the polycrystalline state, hence grain boundaries have always been considered to play an important role in plastic deformation. This role has centered around their ability to act as obstacles to the movement of dislocations. Thus, the classical concept has long been one of yield initiation via dislocation generation in grain interiors and subsequent dislocation pileups against the boundaries causing source activation in the next grain. However, during the past decade, an increasing amount of evidence has established that grain boundaries can also act as dislocation sources, particularly in the early stages of yielding. This region is generally referred to as the premacroyield strain region, and it extends from the first substantial movement of dislocations to the point where massive dislocation movement and multiplication is required to maintain the plastic strain rate imposed by the testing machine. It thus separates the microyield region (plastic strain of zero to around 1×10^{-4}) from the macroyield region (yield point).

The operation of grain boundary sources in the premacroyield region would have a number of consequences:

1) It might affect either the type, character or number per source of dislocations generated,
2) It would affect the work hardening behavior of materials in which cross-slip, and hence tangling, is relatively easy. This behavior would be affected by the changed location of these tangles from

the grain interior to the grain perimeter when boundary sources predominate,

3) The work hardening behavior with respect to solute atoms or particles hindering dislocation movement would be also affected, since solute levels and distribution at the grain boundary can be different from those of the grain interior in many materials.

In addition, the possibility of grain boundaries acting as dislocation sources may have implications for mechanical properties above the yield point, such as creep and fatigue strengths, or the amount of ductility a material possesses.

Although the concept of grain boundary dislocation sources has been formulated for some time, relatively little detailed experimental work has been conducted on their operation or their influence on the yielding process. Therefore this study was directed towards the following objectives:

1) To examine and correlate the many theoretical models for grain boundary structure and grain boundary lattice defects, dislocation nucleation at, and generation from these boundaries, the stresses required for operation of boundary sources and the means of obtaining these stresses,

2) To verify that grain boundary dislocation generation can occur in the premacroyield region of a pure FCC metal (Cu) in which it had not previously been observed, by designing a microstructure conducive to such generation,

3) To develop a method of extracting quantitative data (via electron microscope thin foil examination) concerning boundary source operation,

4) To use this method for measuring relative source densities and distributions in Cu at various strains in the premacroyield region,

5) To study some of the parameters, such as solute content, stacking fault energy, elastic anisotropy and initial boundary defect density, that should influence boundary source operation, by examining selected materials (Cu-1wt%Sn, Ni, Al) in a similar microstructural state to that of the Cu,

6) To examine the characteristics of individual sources in any material, for the purpose of establishing a boundary source model which will account for these characteristics and those determined in 4) and 5).

2 GRAIN BOUNDARY STRUCTURE AND ASSOCIATED CRYSTAL DEFECTS

A grain boundary may be defined as the contact region between two crystals differing only in orientation (1). This definition, although relatively straightforward, sheds little light on the nature of this region, either on the scale of the individual atoms or the larger scale of the various defects present among the arrays of atoms. It is essential to realize that the strength of polycrystals indicates the presence of strong interatomic forces across this region. Thus it is not a "space" between two crystallites (as often represented in drawings) but a transition zone or a special lattice between the two misoriented crystal lattices. It accordingly possesses its own special characteristics, particularly with regard to the interaction of different types of dislocations. The character is also highly variable, and must change as the misorientation changes. This zone is spatially more restricted than our common notion of a lattice, being essentially a two-dimensional film curved so as to surround the grains in three dimensions. This latter point is particularly easy to forget since we are accustomed to observing "ribbons" of grain boundary in transmission electron micrographs.

2.1 GRAIN BOUNDARY PARAMETERS

Before studying the various models which have

been postulated to describe the structure of boundaries, it would be valuable to describe how a boundary is defined with respect to the crystallites it separates. If the crystallites are infinitely large, three angular parameters define their misorientation; one a rotation about an axis normal to the mirror plane separating them (twist component) and two about mutually perpendicular axes within this plane (tilt components). This mirror plane is normally the boundary plane (symmetric boundary), but does not necessarily have to be (e.g. in an asymmetric boundary). For the more normal case of a boundary in a thin foil, two additional parameters describe the orientation of the boundary plane to the foil (2). As shown in figure 1, these are θ, denoting the inclination of the boundary to the foil surface, and ϕ, denoting the angle between the boundary - foil intersection and θ, the misorientation of a common crystallographic direction. This latter parameter encompasses the three angular parameters described above. This normally suffices to accurately reference the boundary, but with the advent of increasingly sophisticated models, Chalmers (3) has recently proposed that an additional three orthogonal inrotational translations are required to describe the relaxation of individual atoms at the boundary. However necessary these may be theoretically, they are as yet of

Figure 1. Geometrical conventions for characterizing a grain boundary (ABCD) in a thin foil of finite thickness, t (after Murr et al, 2).

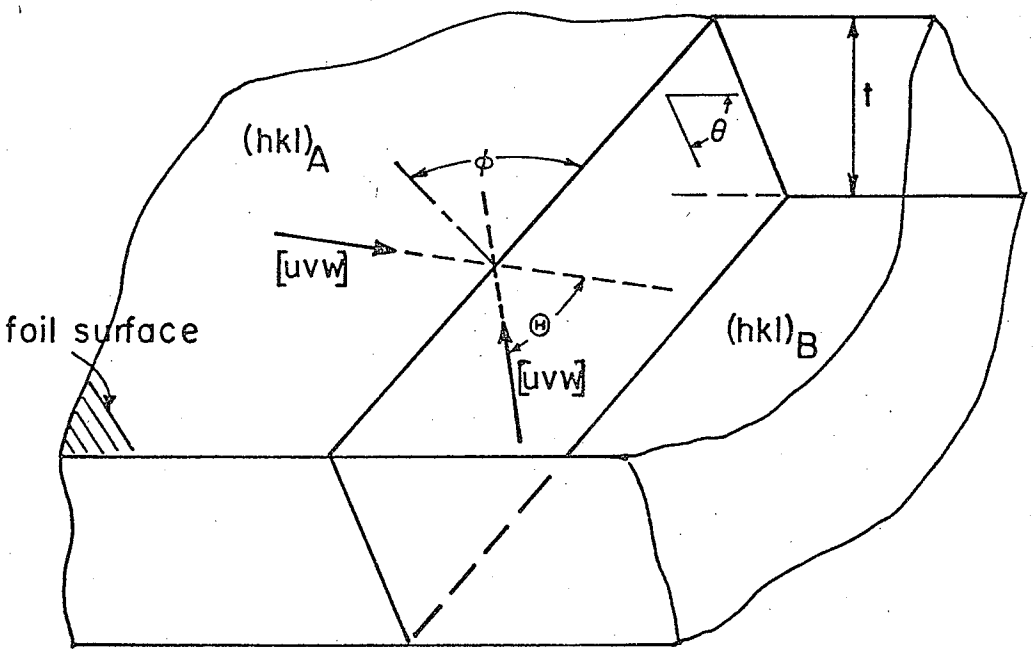
(hkl)A
φ
θ
t
[uvw]
foil surface
Θ
(hkl)B
[uvw]

limited importance experimentally, thus the first five parameters are considered sufficient for most boundary descriptions. It should be pointed out that the above symbols are somewhat confusing in that a great many authors use the lower case theta (θ) to denote the misorientation angle and the lower case alpha (α) to denote the inclination angle of the boundary with the foil surface.

2.2 MODELS OF GRAIN BOUNDARY STRUCTURE

There are two basic approaches to considering models for grain boundaries (4). In one approach the boundary is viewed as a smooth, homogeneous layer purely for thermodynamic purposes. In the other, the basic structure of this layer is described. This study deals with the latter. Gifkin states (4) that a model must satisfy the following criteria to be completely acceptable:

a) it must result in a boundary width of three to four atom diameters to correlate with experimental observations.

b) it must produce a reasonable value of grain boundary energy and the orientation and temperature dependence thereof.

c) it must account for the change in orientation between the two grains while still taking into

account individual atom interactions.

d) it must be able to explain, to at least some degree, a host of properties such as boundary sliding, migration, segregation, corrosion, melting and low temperature mechanical behaviour.

This last requirement is the most difficult to fulfill. The main difficulty to date appears to be that a given model may elegantly account for the behaviour of one or two boundary properties, yet break down completely when the others are considered. For this reason, plus the fact that some models have not yet been evaluated with respect to even the first three criteria, it is impossible to rigorously assess their shortcomings and merits. Thus they will be presented only briefly, with perhaps some indication of current popularity, in order to establish a physical basis for the consideration of dislocation generation from grain boundaries.

One problem endemic to most models is that they were originally constructed to explain the structure of simple "special" boundaries, such as low angle pure tilt or twist boundaries or coincidence boundaries. Ultimately, however, they should be able to give at least an approximate picture of that most common of boundaries in normal materials, the random, high angle (high θ) grain boundary.

2.2.1 AMORPHOUS MODEL

This model, developed by Rosenhain and co-workers (5, 6) was the first real attempt to account for boundary properties. In essence, it considered the boundary as an amorphous, undercooled liquid, i.e. possessing no long range periodic structure. Although this could qualitatively explain such phenomena as grain boundary sliding and brittleness at high and low temperatures, respectively, it has been generally discounted for a number of reasons (1). A calculation of the excess internal energy based on this model leads to calculated values of boundary thickness much larger than observed experimentally. Also, it seems inherently unreasonable that so thin a region would not be influenced at all by the periodic crystal structures on either side of it. Most important, such a model completely fails to account for the variation in many boundary properties with both orientation and/or inclination.

The concept on which the model is based has some value with regard to such matters as calculation of grain boundary energy. Also, as McLean comments (7), the boundary layer bears some similarity to an amorphous layer in that both are regions in which the perfect crystal structure is forbidden, thus tempering somewhat the comparison of this region to a special lattice. Aaron and Bolling (8)

have considered grain boundary energy using somewhat of an amorphous model, that is, the boundary structure with the lowest free volume possesses the lowest energy boundary. They conclude that high angle boundaries are most likely constructed according to a "structureless" model built on the random close-packing of atoms. As we shall soon see, however, there is a good chance that this could correspond to a structured model which allows individual atom relaxation into the lowest energy configuration.

2.2.2 DISLOCATION MODELS

These models consider grain boundaries as planar arrays of dislocations. It is well established that low angle boundaries (9, 10), i.e. low θ values, are composed of arrays of lattice edge dislocations for a pure tilt misorientation, screw dislocations for a pure twist misorientation, or, as is most often the case, dislocations of mixed character for a mixed orientation. This is illustrated in figure 2, with the twist segment on top, the tilt segments on the sides and a mixed segment denoted DCH.

The spacing of these lattice dislocations decreases with increasing misorientation according to $d = \underline{b}/\theta$ (b = Burgers vector, d = spacing), hence the boundary

Figure 2. Illustrating symmetric tilt, twist and mixed low angle grain boundaries for the case of one grain entirely surrounded by another grain, with both sharing a common <001> axis (Bishop and Chalmers, 35).

Figure 3. (a) Dislocation model of a symmetric 53^{o} tilt boundary. (b) Dislocation model of a symmetric 60^{o} tilt boundary (Gleiter, 1).

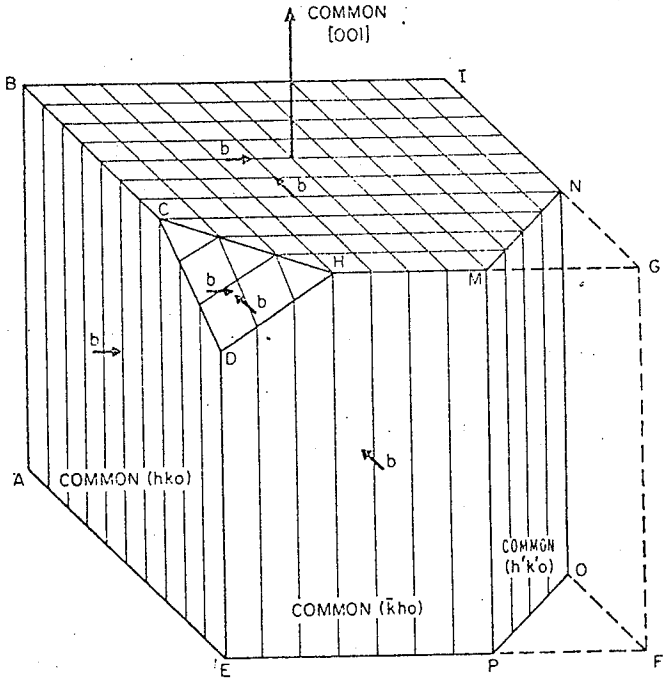
COMMON
[001]
B
T
N
G
C
H
M
D
A
E
P
F
O
b
COMMON (hko)
COMMON (h̄ho)
COMMON
(h'k'o)

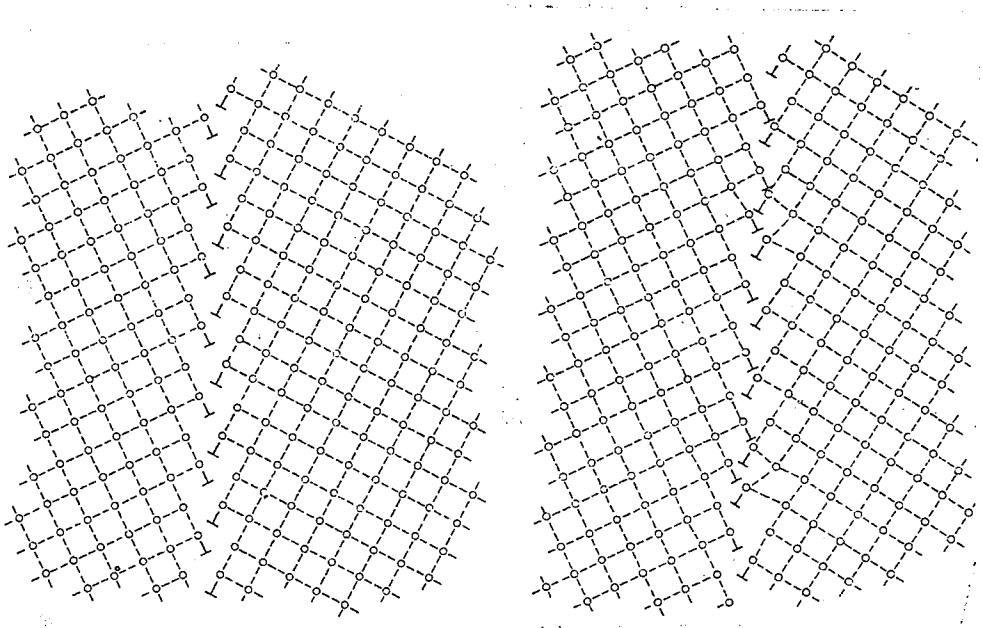

(a) (b)

energy increases with more dislocations per unit length. Up to approximately 15^{o} of misorientation (hence the term low angle boundary), the boundary energy can be accurately calculated from dislocation theory based on linear elasticity. Beyond this point, the dislocation cores become too close to retain their physical identity. The model can be extended on a geometric basis, however (11). This is illustrated in figure 3. The low energy of the 53^{o} tilt boundary of figure 3(a) arises because of the uniform dislocation spacing (one per lattice plane). The higher energy 60^{o} boundary of figure 3(b) may be regarded as a 53^{o} boundary with a 7^{o} low angle boundary superimposed on it. Again, this is only geometrically true, since the two components will interact with regard to the boundary energy. This interaction is almost impossible to calculate because of the physical closeness of the dislocations. More recent models have also discussed boundary structure in terms of dislocations but, because they utilize other concepts as well, they will be presented later.

2.2.3 ISLAND MODEL

This model was first proposed by Mott (12) and later expanded by Gifkins (13) and, as seen in figure 4, it views a grain boundary as consisting of "islands" of

Figure 4. Representation of island model of grain boundaries (with the channels of bad fit shown dashed)
(a) viewed along the boundary plane
(b) viewed normal to the boundary plane (Gifkins, 13).

Figure 5. Coincidence lattice (double circles) resulting from the interpenetration of two crystal lattices (large and small circles). Coincidence lattice unit cell is AOBC and the crystal lattice rotation is shown at right (Fletcher, 29).

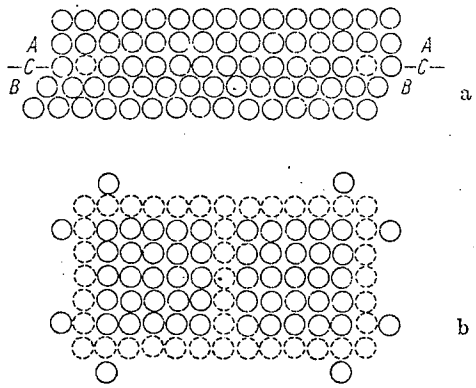
A
C
B
A
C
B
a
b

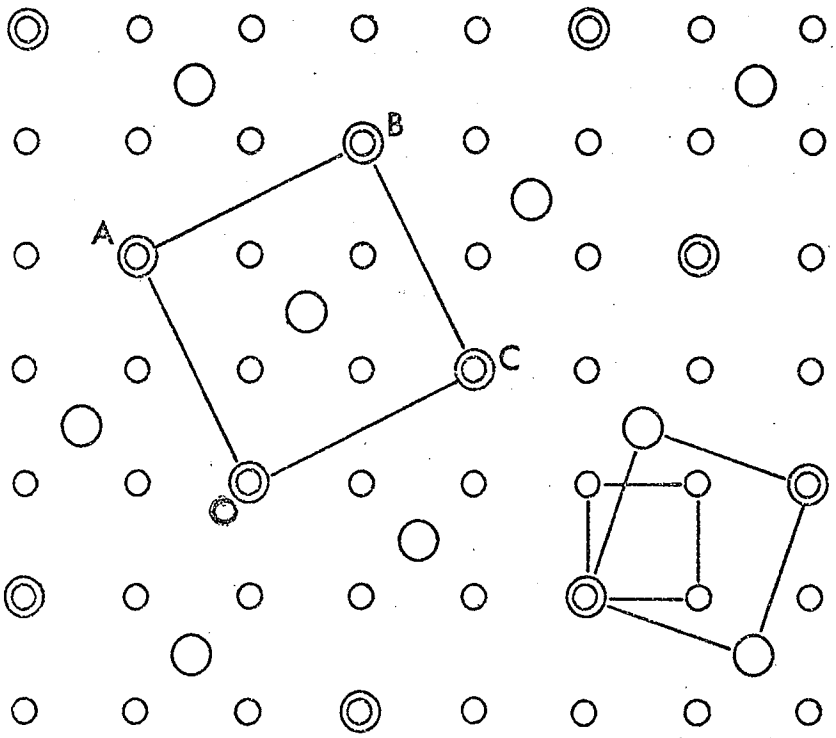
A
B
C

good atomic fit which are surrounded in the plane of the boundary by "channels" of bad fit. These regions have been estimated (13) as varying in size from five to fifty atom diameters (roughly 10 - 100 Å) and thus should be, for the most part, invisible in the electron microscope. They have apparently been seen, in the form of facets, by the field ion microscope (14, 15). Because of the small atomic mismatch across the islands of good fit, short range elastic strains exist which vary in magnitude with the misorientation and account for a minor, but nonetheless significant, portion of the grain boundary energy. Gifkins has stated that these regions of good fit would tend to be oriented so as to permit continuity of slip across them, although this would be very difficult for small island sizes.

The channels of bad fit are essentially relaxed vacancies and can be identified with the ledges on the edges of microfacets, hence the resemblance, as we shall see later, between these regions and grain boundary dislocations associated with ledges. The elastic strains would be much more severe in these channels and despite their smaller area relative to the islands, they are thought to contribute the major portion (roughly 60%) of the total grain boundary energy. The special coincidence boundaries (discussed next) are seen as special cases of this

model where the islands are very large, occupying the entire boundary in the limit of a coherent twin boundary.

Overall, the island model appears to be regarded as a good physical picture of boundary structure, but it has been largely supplanted by more specific models.

2.2.4 COINCIDENCE MODEL

This model hinges on the concept of a coincidence lattice (16, 17), which simply states that when two misoriented crystal lattices are allowed to interpenetrate each other, some of the lattice points will coincide, e.g. O, A, B, C in figure 5. These points form a lattice of larger spacing than either of the original ones, which is called the coincidence lattice for that particular misorientation. The degree of coincidence is denoted by Σ, the reciprocal of the fraction of shared sites, e.g. $\Sigma = 1$ indicates that all sites of the two lattices are shared (coherent twin boundary). For most random orientations about a given axis of rotation, it can be seen that Σ is very large and the concept of coincidence loses much of its utility. For certain orientations, however, the fraction of shared sites becomes very large, and grain boundaries oriented so as to lie along planes of this lattice which possess a high density of shared sites are expected

to have low boundary energies (16). This is due to the absence of long-range elastic strains (much the same as for the "islands" of the previous section. Balluffi and Tan (18) indicate that boundaries with $\Sigma \leq 20$ should fall into this category of a "special" boundary. Although a great deal of experimental work has demonstrated that some amount of energy decrease is achieved for these orientations (roughly 10%), recent work by Dimon and Aust (19) indicates that it can be much larger (30%), while occurring over a very narrow range of orientation. Marked changes in the properties of these boundaries from those of random boundaries was first established by Kronberg and Wilson (20) and has since been well-documented (21). It was further discovered experimentally (22) that deviation of the boundary plane from this low energy plane of the coincidence lattice led to a stepped boundary in order to maximize the amount of boundary lying along the low energy plane. In this fashion, changes in direction of the boundary can be brought about by the proper combination of steps of varying orientations and spacings (figure 6). It should be noted that a similar tendency has recently been demonstrated to occur on a much larger scale, i.e. for large grain boundary facets (23).

For small deviations from the exact coincidence

Figure 6. Grain boundary curvature effected by variation in step orientation and dimensions. TP = boundary triple point, K = boundary kink (Murr et al, 2).

Figure 7. Illustrating the creation of boundary dislocations due to orientation deviation from exact coincidence.
(a) 53^{o} tilt boundary about [001] - low Σ
(b) creation of $\frac{a}{10}$ [310] boundary dislocation due to 3^{o} deviation (Bishop and Chalmers, 35).

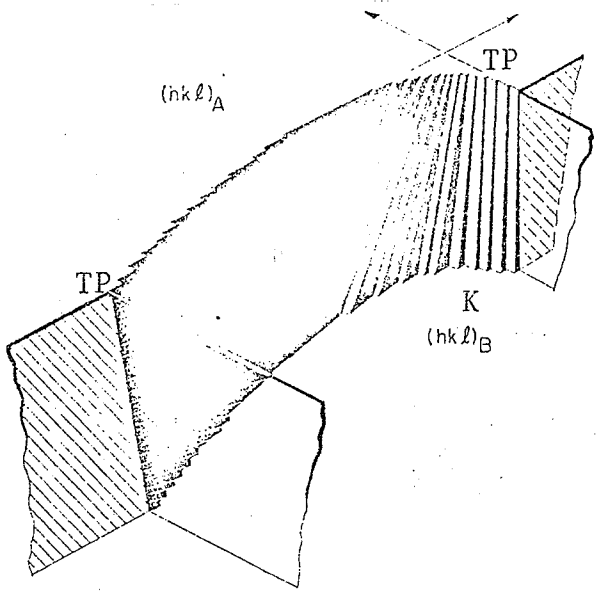
TP
$(hk\ell)_A$
TP
K
$(hk\ell)_B$

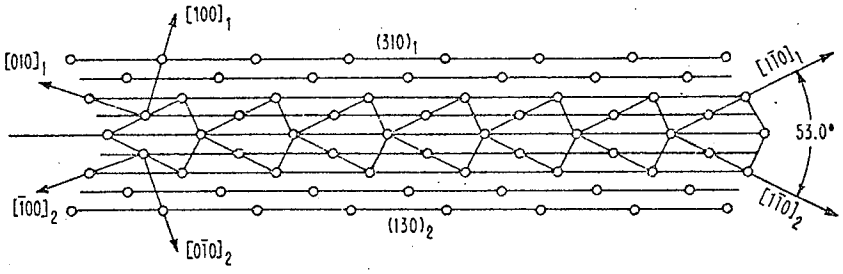
$[100]_1$
$(310)_1$
$[010]_1$
$[1\bar{1}0]_1$
53.0°
$[\bar{1}00]_2$
$[1\bar{1}0]_2$
$(130)_2$
$[0\bar{1}0]_2$

(a)

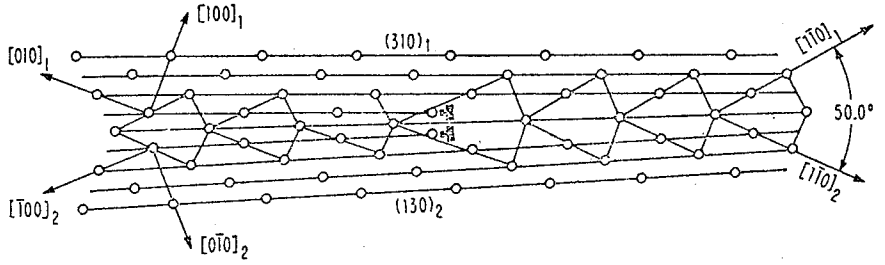
$[100]_1$
$(310)_1$
$[010]_1$
$[1\bar{1}0]_1$
50.0°
$[\bar{1}00]_2$
$[1\bar{1}0]_2$
$(130)_2$
$[0\bar{1}0]_2$

(b)

orientation (a few degrees), the boundary may be returned to the low energy orientation by imposing a dislocation network on the boundary which amounts to a sub-boundary of the coincidence lattice (22, 24). An example of such a dislocation is shown in figure 7 for a simple tilt boundary. The Burgers vectors of these dislocations (as for all boundary dislocations) may be derived from the DSC lattice of Bollmann (17). This lattice consists of all possible translations of one crystal lattice with respect to another. Thus, unlike the coincidence lattice which deals only with shared sites, the DSC lattice deals with all sites. Figure 8 illustrates this for a simple 36.9^{o} tilt boundary about <001>. The two interpenetrating lattices are shown (one open circles, one solid) and a cell of the coincidence lattice, ABCD. The primitive or base vectors of the DSC lattice, $\overline{b}_1$, $\overline{b}_2$, $\overline{b}_3$ indicate that a translation of the solid circles with respect to the open circles by any of these amounts (or multiples thereof) results in an identical configuration. In this sense, $\overline{b}_1$, $\overline{b}_2$ and $\overline{b}_3$ represent the smallest possible Burgers vectors for perfect grain boundary dislocations. The DSC lattice is simply constructed by drawing an orthogonal network through all lattice sites. The base vectors are then the shortest translations between sites in the three orthogonal directions. The DSC lattice is derived, in turn, from

Figure 8. DSC and coincidence lattice for a 36.9° tilt boundary about [001]

(a) viewed parallel to the rotation axis

(b) showing the three base vectors of the DSC lattice (Balluffi et al, 47).

Figure 9. Illustrating the O - lattice, similar to the coincidence lattice (AOBC), but supplemented by additional non - lattice points (such as O') about which the two interpenetrating lattices may be rotated with respect to each other (Fletcher, 29).

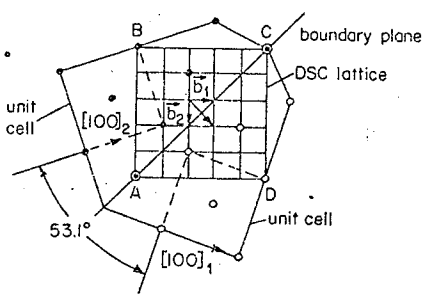
B
C
boundary plane
DSC lattice
unit cell
$[100]_2$
$\vec{b}_1$
$\vec{b}_2$
A
D
unit cell
53.1°
$[100]_1$

(a)

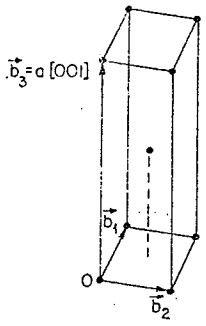
$\vec{b}_3$=a [001]
$\vec{b}_1$
O
$\vec{b}_2$

(b)

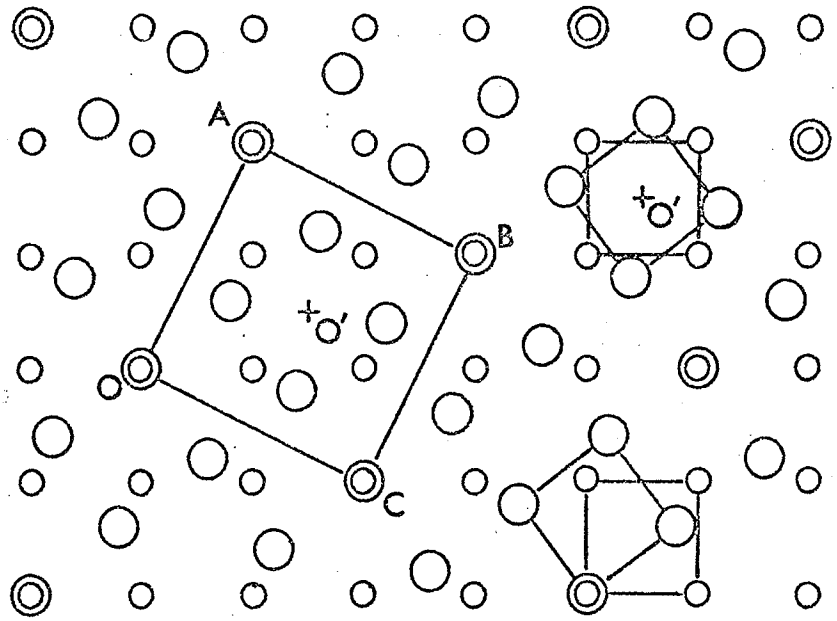
A
B
C
O'
O'

Bollman's generalized O - lattice (figure 9).

Although it somewhat resembles a coincidence lattice, the O - lattice is far more flexible as it permits crystal lattice translations about points in its lattice which are not crystal lattice sites, e.g. O' in figure 9. This occurs when the translation of one crystal lattice with respect to another is by a non - DSC vector (25). This would result in the breakdown of the coincidence model, but, as stated, the O - lattice merely shifts its lattice points off those of the crystal lattice. The significance of this is that virtually any boundary can be geometrically characterized even though its detailed physical structure is unknown.

These boundary dislocations have been experimentally observed (26, 27, 28) but only with difficulty, and for small deviations from coincidence. This is caused by two factors. First, the spacing of the dislocations is very sensitive to deviation from coincidence due to the relatively small values of Burgers vectors. These Burgers vectors decrease with increasing Σ (29), i.e. as the coincidence lattice becomes larger. Thus the dislocations are very close together even for orientations only a degree or so from exact coincidence. Second, the reduced Burgers vector results in poor electron microscope contrast due to the reduced strain field. Thus, Balluffi and Tan (18) have

recently proposed that such networks may be present over the entire misorientation range, only they cannot possibly be resolved. In such a case, it would be difficult to consider them in the normal physical sense of a dislocation network.

One final point of importance is that, while coincidence boundaries can account for a substantial fraction of all possible misorientations (24), there is no particular reason that they have to. That is, grain orientations are set either from nucleation in the melt or recrystallization nuclei, and not from energetic considerations which would only be realized when they begin to meet and form grain boundaries. Thus, Loberg et al (15) found no particular preference for exact coincidence orientations in a review of field ion microscope orientation determinations. One factor that could modify this randomness in the direction of more coincidence boundaries is that of texture, since this will at least orient grains so as to possess a common pole of low crystallographic index, which is essential to high degrees of coincidence. Also, it bears emphasis that, for a given orientation, the grain boundary will tend, through boundary migration and/or annealing twin formation, to lie along the lowest energy plane of the coincidence lattice for that orientation. The difference for different orientations is purely one of degree, since the reduction in

energy will be greatest for the high coincidence orientations.

2.2.5 STRUCTURAL UNIT MODEL AND OTHERS

One of the major weaknesses in the coincidence model is that the geometric requirements of lattice coincidence are quite rigid, i.e. the density of coincident sites drops precipitously when the misorientation moves even slightly away from exact coincidence. On the other hand, the change in properties which is characteristic of these boundaries often persists up to several degrees from exact coincidence (1). This led Bishop and Chalmers (30) to propose their "coincidence - ledge - dislocation" model of boundary structure which has subsequently evolved into the well-known structural unit model (1, 31, 32). The critical difference in this model is that it stresses boundary coincidence, i.e. sharing of atoms along the boundary plane, rather than lattice coincidence. As summarized by figure 10, an exact coincidence boundary (figure 10a) may thus be viewed as constructed of microledges of equal width (figure 10b). It may also be viewed as a "shared atom" configuration (figure 10c) or, alternatively, as a "translated" one (figure 10e). The array formed by the shared atoms of figure 10(c) is shown in figure 10(d), and the variation in the make-up of the structural units with misorientation is shown in figure 10(m).

Figure 10. Coincidence - ledge - dislocation representation of (a)-(f) 28.1° exact coincidence tilt boundary about [001] (g)-(l) 29.4° off - coincidence tilt boundary about [001] (m),(n) structural units for low Σ boundaries (Bishop and Chalmers, 30).

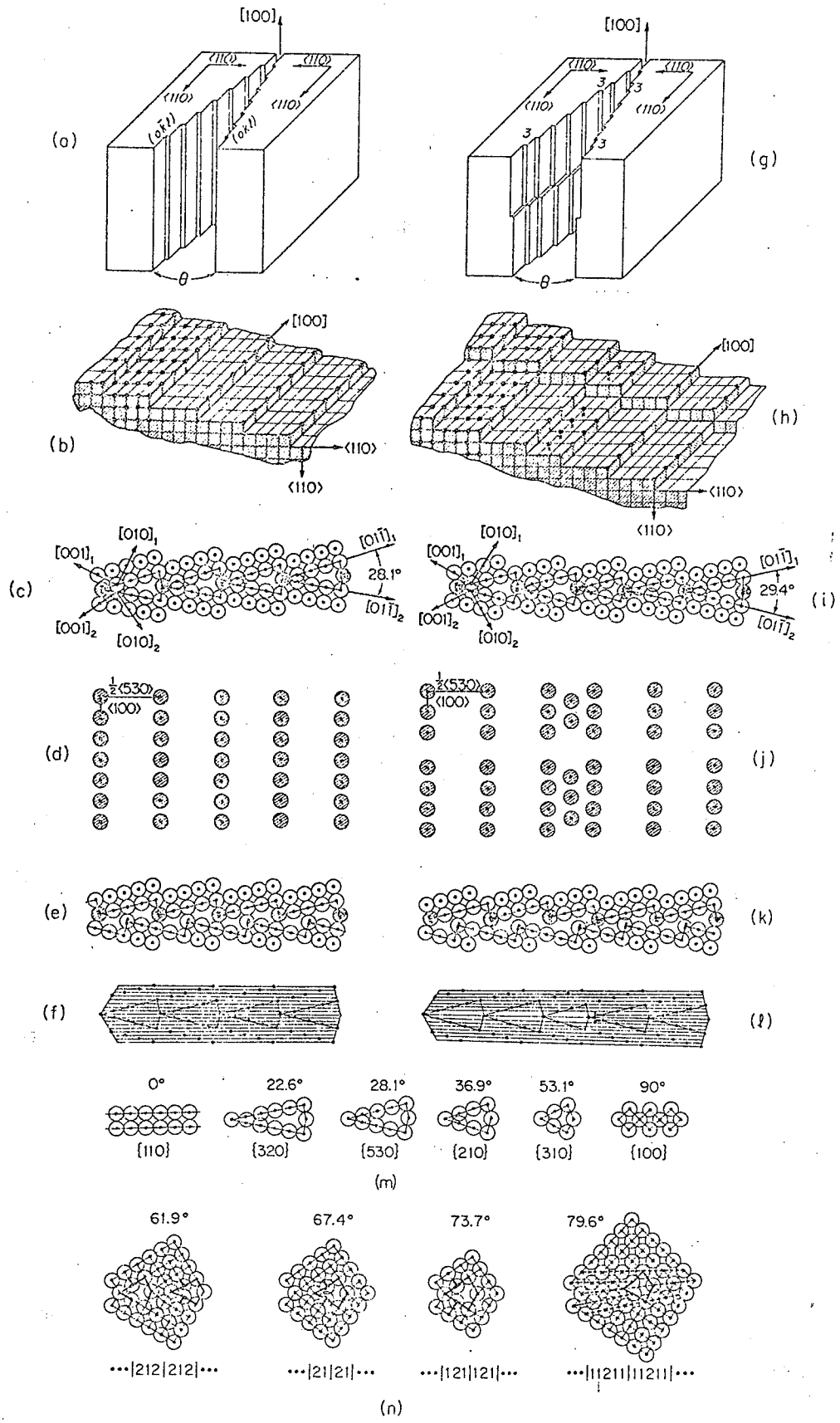
(a)
[100]
⟨110⟩
⟨110⟩
⟨110⟩
⟨110⟩
(0k̄l)
(0kl)
θ
(g)
[100]
⟨110⟩
⟨110⟩
3
3
3
3
⟨110⟩
θ
(b)
[100]
⟨110⟩
⟨110⟩
(h)
[100]
⟨110⟩
⟨110⟩
(c)
[010]₁
[001]₁
[01$\bar{1}$]₁
28.1°
[001]₂
[010]₂
[01$\bar{1}$]₂
(i)
[010]₁
[001]₁
[01$\bar{1}$]₁
29.4°
[001]₂
[010]₂
[01$\bar{1}$]₂
(d)
½⟨530⟩
⟨100⟩
(j)
½⟨530⟩
⟨100⟩
(e)
(k)
(f)
(l)
0°
22.6°
28.1°
36.9°
53.1°
90°
{110}
{320}
{530}
{210}
{310}
{100}
(m)
61.9°
67.4°
73.7°
79.6°
•••|212|212|•••
•••|21|21|•••
•••|121|121|•••
•••|11211|11211|•••
(n)

The units are designated in terms of the ledge lengths expressed as multiples of a/2 <110> (for this case), e.g. "3" for the 36.9° structural unit of figure 10(m). Deviations from exact coincidence are simply achieved by a mixture of the units from the two nearest exact coincidence orientations. Thus, for a 29.4° boundary, shown in figure 10(g-l), this results in four - "4" units followed by one "3" unit, i.e. a straight proportional mixture. For higher misorientations, the boundaries are mixtures of "2" ledges and an increasing number of "1" ledges (which are essentially regions of single crystal). These are shown in figure 10(n). In this fashion the boundary coincidence is high even though the lattice coincidence is low. Extra deviations (tilt or twist) result in additional ledges (figure 10g, h). The concept of the model in terms of dislocations arises from viewing any row of atoms ending at the boundary as the extra half plane of a dislocation, e.g. figure 10(e) or 10(k). It can be seen that the perturbations resulting from off-coincidence orientations (figure 10j) can be regarded in the same light as the coincidence lattice sub-boundary networks. These perturbations (dislocations) have the important effect of creating a long-range stress field at the boundary, with the extent being comparable to the distance between the perturbations (30). There is even a limited resemblance to

the island model in that the minority structural units of an off-coincidence boundary may be regarded as the bad fit regions (high strain) around the regions of good fit (low strain), although the two concepts are dimensionally different, one linear and the other, an area.

In recent years, this model has undergone further development by consideration of the structural units in terms of free energy as well as geometry. Thus Chalmers and co-workers (31, 32) have considered individual atomic displacements through computer calculations. (It should be noted that a similar consideration was undertaken by Baroux and co-workers (33, 34), but only in the geometric sense). The rationale leading to this consideration arises from the strength of grain boundaries. Since substantial numbers of dislocations can pile up against boundaries without penetrating through them, their strength should at least be of the same order as that of the perfect crystal (1), yet the shared fraction of atoms is relatively small, even for unrelaxed models. This localized relaxation results in an overall energy decrease (figure 11 - where $E(a) > E(b) > E(c)$), even though a trade-off is involved because of the addition of long-range elastic distortion. It is essential to realize that such relaxation will destroy all coincidence at the boundary. In this model, asymmetrical boundaries are

Figure 11. (a) 38^{o} tilt boundary - rigid structural unit model
(b) same boundary allowing crystal translation for energy reduction
(c) same boundary allowing individual atom relaxation for energy reduction (Gleiter, 1).

Figure 12. Asymmetrical 29^{o} tilt boundary about [001], composed of symmetrical segments DE, EF and FG (Chalmers and Gleiter, 32).

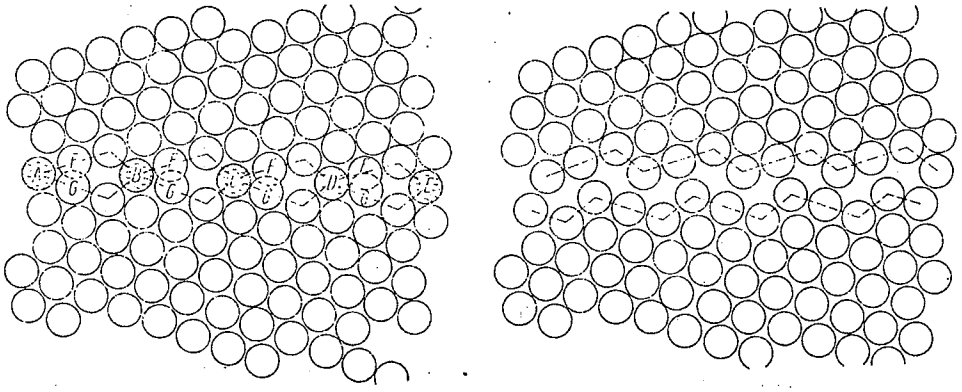

(a) (b)

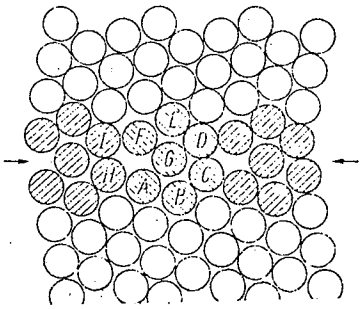

(c)

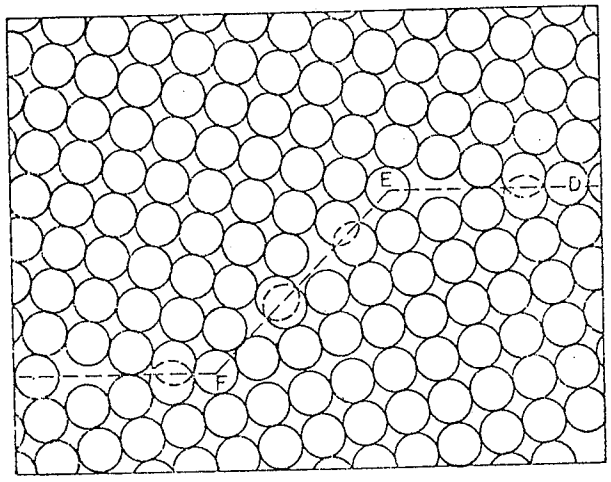

simply constructed by stepped segments of symmetrical boundaries, each with its own mixture (if need be) of structural units (figure 12).

Mention should be made of two very recent grain boundary models which, like the structural unit model, attempt a multi-faceted approach at describing the structure. In the planar matching model (36, 37), the basic premise is that families of atomic planes which meet at the boundary so that their traces are only slightly mismatched, will give rise to boundary dislocations similar to interfacial dislocations between two phases which are partially coherent (37). Another way of viewing these is to consider the slight mismatch of equi-spaced grids as producing a Moiré pattern in which the Moiré lines are lines of relatively bad atomic fit, i.e. dislocations (36). These dislocations would be somewhat different from the off-coincidence networks discussed earlier, especially in the fact that their spacing would be much less sensitive to deviation from a symmetric orientation (where the planes matched perfectly) and that their Burgers vectors would always lie in the boundary plane (37). Although the theory experimentally has been seen to account for some boundaries (38, 39), there is some question whether it can account for all boundaries (40), as a general model should. In addition, the model works best

when the matching planes are of low index, i.e. atomically smooth (37), and it could be questioned whether this is a reasonable assumption for random high angle boundaries.

The other model of Marcinkowski and co-workers is a coincidence-dislocation approach to boundary structure (41). The major premise is that all boundaries can be regarded as being composed of dislocations, said dislocations being regarded as various combinations of crystal lattice dislocations. For exact coincidence orientations, these lattice dislocations are visualized as coming from the primary slip planes of both grains, and the coincidence site lattice (denoted the primary coincidence lattice) is identical to that discussed previously. For off-coincidence orientations, lattice dislocations are visualized to come into the boundary from secondary slip planes also. It is shown that a new, larger coincidence lattice results (denoted the secondary coincidence lattice). The model takes issue with the Bollmann formulation for grain boundaries (17) in stating that boundaries can only be constructed in discrete fashion, i.e. as integral functions of the number of lattice dislocations used and the spacings of the slip planes used, and <u>not</u> in a continuous manner as the 0 - lattice approach allows. Hence the generation of specific coincidence lattices, primary and secondary. The model has been formulated

for both symmetric (42) and asymmetric (43) tilt boundaries, and for twist boundaries (44), in both ordered and disordered simple cubic lattices. In addition it has been extended for the above cases to the body-centered cubic lattice (45) and experimental observations of boundary dislocation networks have been conducted on a FeCo alloy with this structure (46). Much as in the planar matching model, this model thus furnishes a possible explanation for such networks which are very regular and spread over the entire boundary, yet have far too great a spacing to be the aforementioned off-coincidence sub-boundaries. However, as with the earlier, simpler dislocation models, there still remains the fact that, by and large, these boundary dislocations can only be considered geometrically and not physically. Thus, while these recent models are being assessed (and likely refined), the revised structural unit model appears currently to be the most acceptable for generating the best overall picture of the actual structure of the boundary, energetically, geometrically and physically. This picture appears to be moderately clear for relatively simple boundaries and is furnishing at least a dim outline of even the most random boundary. It would be appropriate at this point to consider the crystal defects associated with this basic structure.

Leaf blank to correct numbering

2.3 GRAIN BOUNDARY DEFECTS

2.3.1 TERMINOLOGY

As with any field which experiences a sudden surge of interest and new growth, there has been a proliferation in the terminology pertaining to grain boundaries which reflects the increasing sophistication with which this region has been studied. Unfortunately, the evolution of this terminology has been anything but orderly.

The topography of grain boundaries is moderately clear. Triple points generally refer to the intersections of three grain boundaries (figure 6, p.17) but can be used to describe twin boundary - grain boundary intersections. Large, relatively sharp changes in boundary curvature have been sometimes called kinks (k in figure 6) and are generally a consequence of limited grain growth. Small scale boundary curvature, such as shown in figure 6, is brought about by steps and/or ledges. The ledge is normally considered to be the longer of the two but, as is apparent by now, many authors use the two interchangeably. At the same time, these features are generally larger than the steps/ledges evident on even the most planar portions of boundary, e.g. figure 10 (p23). No real distinction appears to have been made between the two, so henceforth the latter will be termed microsteps or microledges.

The one boundary defect which has a counterpart in the grain interior is the grain boundary dislocation (GBD) and it is here that the terminology has run rampant. Brandon et al (22) referred to off-coincidence boundary dislocations as a dislocation sub-boundary. Schober and Balluffi (26, 27) have referred to them as intrinsic GBD's and McLean (7) has called them structural dislocations. To Bishop and Chalmers (35) they were secondary intrinsic GBD's (primary intrinsic GBD's were those forming exact coincidence boundaries). Brandon (24) discussed step dislocations, i.e. those associated with boundary steps, whereas Ishida et al (48) simply call these grain boundary dislocations, a term which they also apply to those making up the boundary structure and any lattice dislocations which have impinged upon the boundary (49). Similar "blanket" definitions have also been used by Bell and Langdon (50) and Ashby (51). Gleiter et al (52) used GBD only to denote boundary dislocations generated within the boundary. These and any other dislocations superfluous to the boundary structure were referred to by Schober and Balluffi first as extraneous GBD's (53), then as extrinsic GBD's (47). McLean (7) mentions intergrain dislocations in much the same context. Malis et al (54) have subdivided extrinsic dislocations into primary extrinsics (referring to those resulting from lattice dislocation - intrinsic GBD interactions) and secondary extrinsics (referring to those

produced in the boundary).

Marcinkowski (55) has defined the dislocations resulting from lattice dislocations cutting through the boundary as virtual grain boundary dislocations (VGBD's), meaning that they possess a stress field but no definable Burgers vector, although he has since reconsidered this assignation (57). Some authors have regarded boundary dislocations and steps as essentially equivalent (2) but there are important differences. As Ashby notes (51), movement of a true step produces boundary migration without relative displacement of the two grains, whereas GBD movement does. A step is a poor source or sink of vacancies while a GBD can be a good one. Furthermore, a GBD can interact strongly with solute stoms whereas a step generally does not (having a much weaker strain field). Finally, McLean (7) has proposed two overall structures for the grain boundary region - the general structure (that which brings about the misorientation between the two grains) and the defect structure (consisting of everything else associated with the boundary). This is a useful division for, as shall be seen shortly, it is the defect structure which appears to play the major role in dislocation generation from grain boundaries.

The confusion in terminology has been at least

partially cleared up by Hirth and Balluffi (56). They have proposed that any dislocation lying in a boundary be denoted a GBD. The one major exception to this blanket definition is for those dislocations forming the intrinsic structure of the boundary, i.e. those which bring about the misorientation. These are denoted intrinsic GBD's (IGBD's). As shown in figure 13, the Burgers vector of a GBD may be determined from a Frank circuit, the familiar circuit based on a lattice surrounding the defect in question. In the case of a GBD this is the coincidence lattice. Figure 13 illustrates this for a coherent twin boundary in the FCC lattice (for simplicity). Figure 14 illustrates what Hirth and Balluffi call a Read circuit, which can be based either on individual crystal lattices or suitably rotated DSC lattices. The closure failure in either case represents the total IGBD Burgers vector content of that portion of the boundary within the circuit, although this total may be decomposed in different ways, e.g. figure 14a where F_1F_2 can be decomposed in two ways. This may sound confusing, but it must be remembered (as emphasized earlier) that these are geometric equivalents only, hence the flexibility in partitioning the total Burgers vector content. When a GBD is present (figure 14 b or c), the closure failure gives the IGBD content plus the GBD Burgers vector. In such cases the IGBD content of a boundary can only be determined

Figure 13. (a) Coherent twin boundary in the FCC structure
(b) containing a Shockley twinning dislocation
(c) containing a pure ledge
(d) containing a GBD with Burgers vector normal to the boundary.

The Frank circuits are denoted $S_1F_1F_2S_2$ and two cells of the coincidence lattice are shown, as well as the DSC - lattice (Hirth and Balluffi, 56).

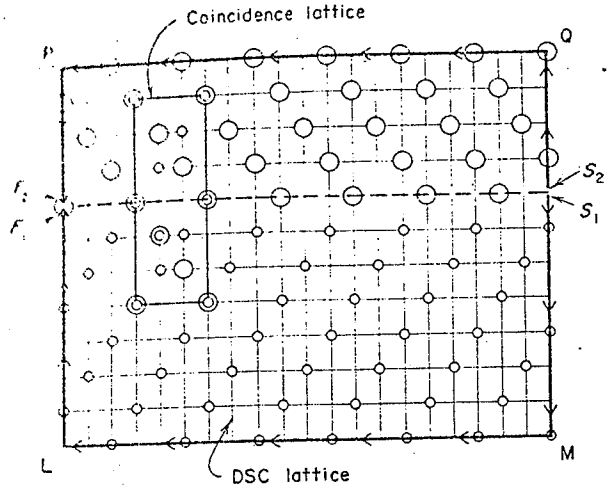
Coincidence lattice
P
Q
S_2
S_1
L
M
DSC lattice

(a)

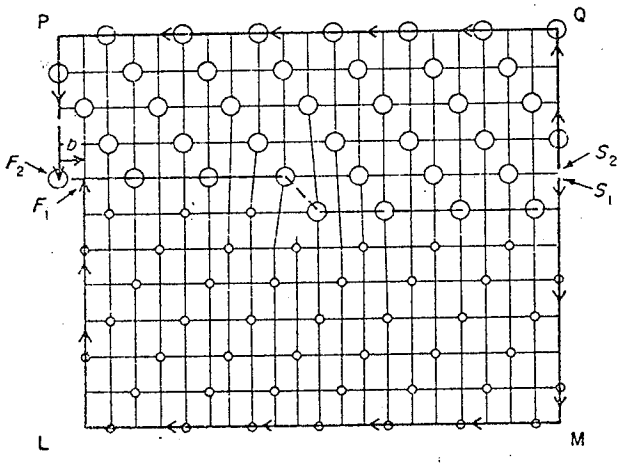
P
Q
b
F_2
F_1
S_2
S_1
L
M

(b)

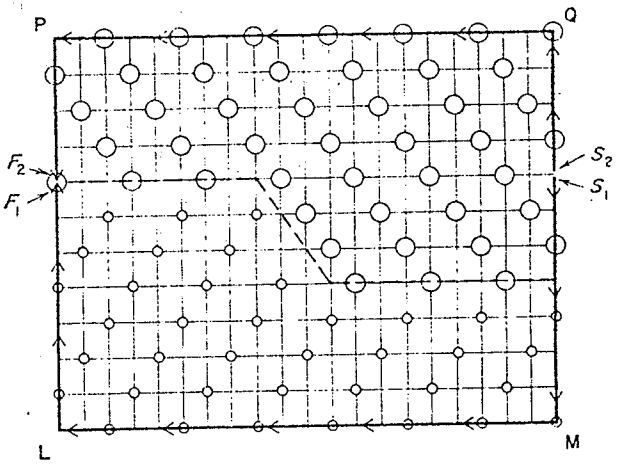
P
Q
F_2
F_1
S_2
S_1
L
M

(c)

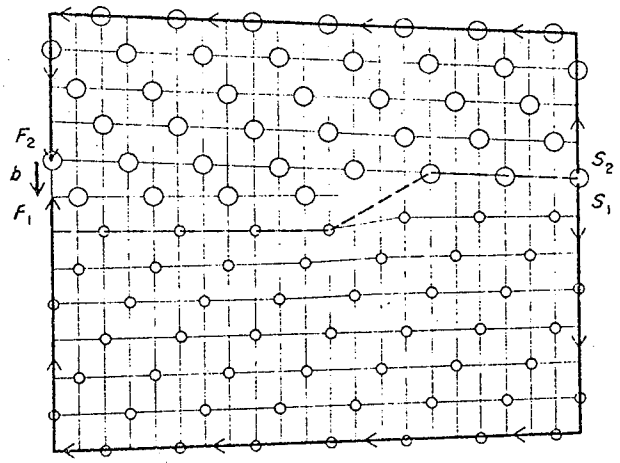
F_2
b
F_1
S_2
S_1

(d)

Figure 14. As figure 13 except that rotated DSC - lattices for each grain are shown, and Read circiuts based on the DSC - lattices (solid lines) and crystal lattices (dashed lines) are also indicated.

(a) Demonstrates how the total Burgers vector content (F_1F_2) may be regarded as four $\frac{a}{3}$ [111] IFBD's (spacings in the common DSC - lattice normal to the boundary) or six $\frac{a}{6}$ [112] IGBD's (spacings along the individual rotated DSC - lattices) (Hirth and Balluffi, 56).

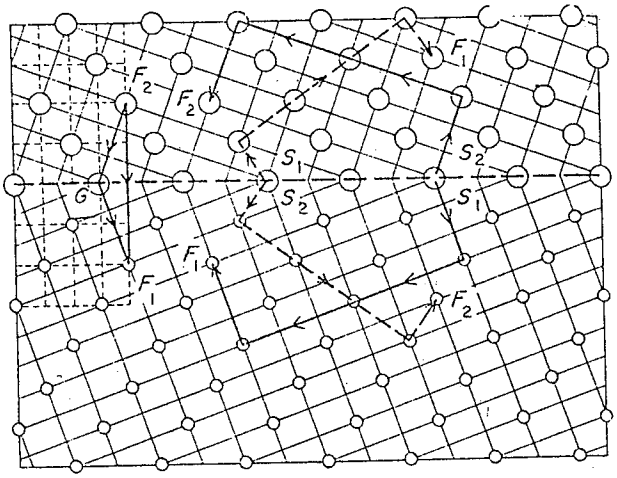

(a)

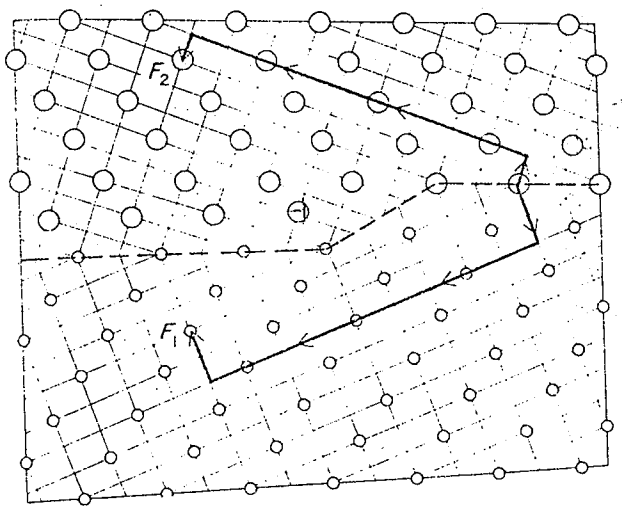

(c)

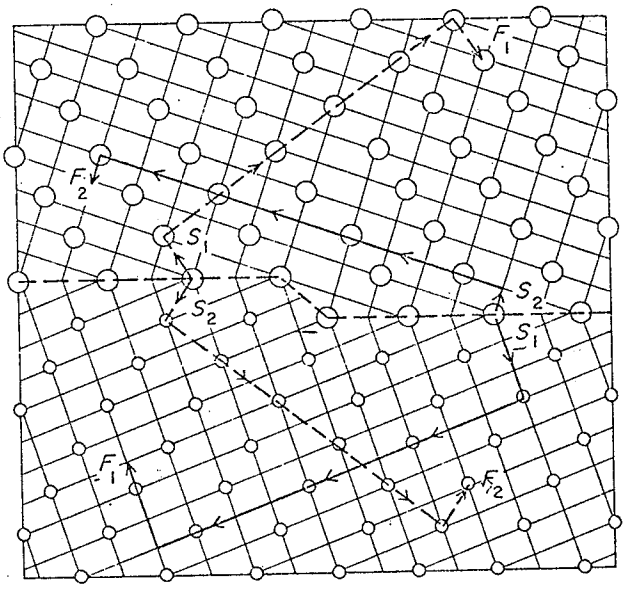

(b)

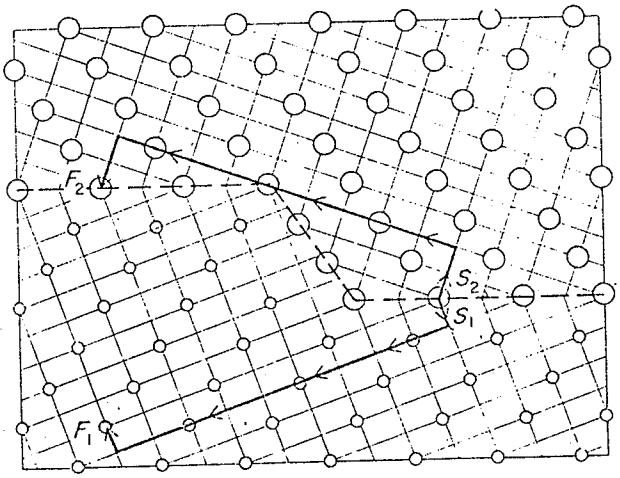

(d)

by constructing both Frank and Read circuits and taking the difference.

The second major classification of Hirth and Balluffi was to denote boundary dislocations as either primary or secondary, where primary refers to lattice Burgers vectors and secondary to any other Burgers vectors of the DSC - lattice. Thus the twin boundary dislocations of figure 13(b) and (d), IGBD's of low angle boundaries and some GBD's resulting from lattice dislocations impinging upon boundaries (53) are classified as primary.

It has become an established experimental fact that boundary steps can have GBD's associated with them (22, 48), e.g. when the step height is not an integral multiple of the coincidence lattice spacing (figure 15). Hirth and Balluffi have extensively categorized this situation. They first define a monatomic climb ledge (C - ledge) associated with a GBD whose Burgers vector is normal to the boundary. As shown in figure 16(c) and (d), the ledge character of the GBD (actually the extra half plane) arises because its climb along the boundary either expands or contracts the volume of the grain it lies upon. Glide ledges (G - ledges), also monatomic, are those associated with GBD's whose Burgers vectors are parallel to the boundary. The glide character arises because of the fact that the ledge movement (figure 16 (e) and (f)) takes place merely by

Figure 15. (a) C - ledge with Burgers vector normal to the boundary

(b) G - ledge with Burgers vector parallel to the boundary

Note that the step height is not an integral multiple of the coincidence lattice unit cell (large squares) (Darinskii and Fedorov, 58).

Figure 16. (a),(b) Construction of a reference bicrystal containing a defect - free grain boundary.

(c),(d) Introduction of a GBD with C - ledge character.

(e),(f) Introduction of either a pure ledge or a GBD with G - ledge character (Hirth and Balluffi,56).

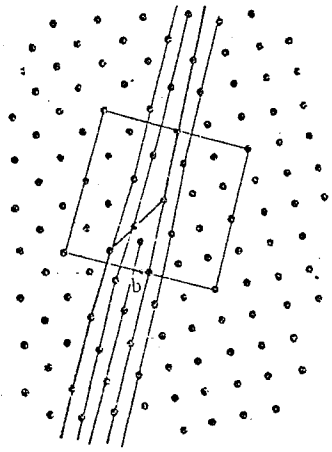

(a)

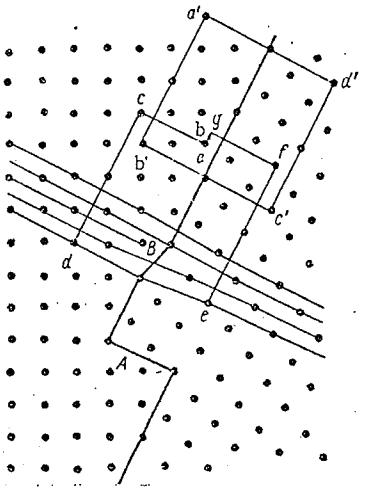

(b)

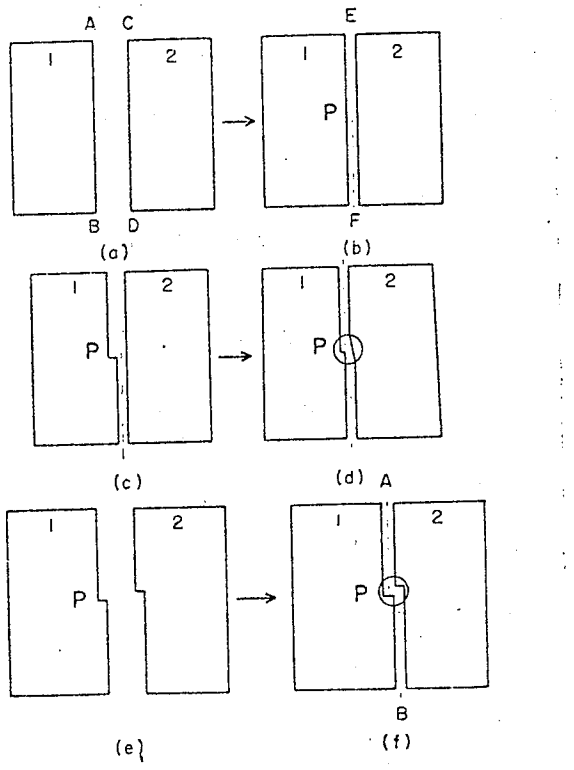

transferance of atoms from one crystal to the other. A pure ledge results (figure 16 f) when no displacement between the matching ledges occurs (no associated Burgers vector). A pure GBD may occur for the case of figure 16(b) when a localized displacement parallel to the boundary occurs that has no accompanying ledge characteristics. Thus figure 15(a) would be a GBD with C-ledge character and figure 15(b) would be a GBD with G-ledge character. A summary of the defects defined by Hirth and Balluffi is given in Table 1.

In addition, we will define a GBD-macroledge as an association of any GBD with a step of greater than monatomic height (such as if the G-ledge of figure 15(b) moved to the step, A). This distinguishment must be made since the GBD-macroledge would be much less mobile than either the C-ledge or G-ledge, even at elevated temperatures.

2.3.2 DIFFRACTION CONTRAST AND OTHER ASPECTS

The diffraction contrast of GBD's is rather complex, since the strain field extends into both grains, and no universally acceptable means of Burgers vector determination has evolved to date. Some contrast effects can be used to distinguish between various boundary defects. Gleiter (59) observed that pure steps showed very weak

TABLE 1

GRAIN BOUNDARY LINE DEFECTS AND CIRCUITS FOR REVEALING THEM (after Hirth and Balluffi,56)

ENTITY	DESCRIPTION
Grain boundary dislocation (GBD)	Any dislocation lying in a grain boundary. Its Burgers vector is a vector of the DSC-lattice.
Climb ledge (C-ledge)	A grain boundary ledge associated with a GBD which requires climb to move in the boundary plane.
Glide ledge (G-ledge)	A ledge associated with a GBD which may glide in the boundary plane.
Pure ledge	A ledge with no associated GBD.
Intrinsic grain boundary dislocation (IGBD)	A GBD which is part of the boundary structure and therefore does not possess a long-range stress field.
Frank circuit	Modified Burgers-type circuit for revealing GBD's
Read circuit	Modified Burgers-type circuit for revealing both GBD's and IGBD's.

Note: It is important to remember that the C- and G- designation refer to the dislocation movement in the boundary plane only. Thus they should not be confused with the dislocation's movement in the grain interior,i.e. a C-ledge will glide into the grain interior,but climb in the boundary plane.

contrast (due to their small strain field), a contrast which did not change noticeably with tilting. GBD's, on the other hand, can be made to disappear quite readily and their contrast can be quite strong, depending on the magnitude of their Burgers vector. Ishida and Henderson-Brown (49) noted that GBD's showed a contrast reversal from black to white when tilted from a strong operating reflection to its negative. They further maintained that this would also apply to dislocations adjacent to the boundary, presumably because their strain field would extend into the adjacent grain. Thus there is likely to be a definite zone around the boundary proper in which lattice dislocations will be indistinguishable from GBD's. With regard to the contrast reversal, McDonald and Ardell (60) have discovered that it does not occur when the strongly diffracting grain is on the lower side of the boundary plane in a thin foil (this would be the left-hand grain in figure 1), thus the above criterion should be used cautiously in separating GBD's from lattice dislocations. McDonald and Ardell also note that an indicator of the strong two beam condition in only one grain is an attenuation in the boundary fringes toward the thick end of the boundary wedge, i.e. if the two beam condition was operating in the left-hand grain of figure 1, the fringes would disappear towards AB. Deviation from such a condition would result in the normal

boundary contrast with fringing at both top and bottom and attenuation in the center. The importance of this lies in the fact that high contrast micrographs of GBD's for studying fine details, are best obtained in the dark field of the strong two beam case, e.g. (46).

IGBD Burgers vectors are generally small and their contrast quite weak (26, 27), but Ishida and McLean (61) have recently suggested that the Burgers vectors of IGBD's in random high angle boundaries should approach lattice Burgers vectors. They calculated the three base vectors of the DSC-lattice (figure 8b, p.19) for various FCC and BCC grain misorientations. They found that, as Σ increased (i.e. tending toward more random orientations), $\underline{b}_1$ and $\underline{b}_2$ decreased while $\underline{b}_3$ approached the interplanar spacing of the planes normal to the misorientation axis. Thus, for symmetrical boundaries, the IGBD Burgers vector would lie in the plane of the boundary, as in the planar matching model. This works quite well for low index misorientation axes, but would not seem to be of much significance for high index ones. Visual confirmation of this hypothesis would be difficult because of the close spacing for IGBD's. Nevertheless it is difficult to believe that these IGBD's would be those seen in "normal polycrystalline specimens", as Ishida and McLean suggest. If that were the case, boundaries even in annealed material would be expected to

show a very high GBD density. There is field ion microscope evidence that IGBD's with lattice Burgers vectors exist, e.g. $\frac{a}{3}$ <111> IGBD's in BCC tungsten (62), but it is to be remembered that boundaries in such specimens are highly textured and are not totally representative of normal polycrystals.

If, in some cases, IGBD's and GBD's can individually show similar contrast, the same would apply to the GBD-macroledge configuration. One therefore has to examine both the shape and density of the defects. Figure 17 shows what this author believes to be reasonably clear examples of these defects (in agreement with the authors of the studies). Thus strong contrast, irregular spacing and curvature indicate the defects of figure 17(a) are likely pure GBD's. The boundary dislocations of figure 17(b) are more regularly spaced, but still relatively far apart. This separation plus the strong contrast and curvature, favor them to be GBD's. The faint network of background defects (fine lines running almost vertically) is almost certainly of IGBD's because of their close and very regular spacing and weak contrast. In figure 17(c) the large fringe shifts, straightness of the defects and semi-regular spacing indicate a pure ledge character, the strong (in part) contrast and spacing variation in different boundary segments rule out IGBD's, hence the conclusion that they are GBD-macroledges.

Figure 17. (a) Pure GBD's in a grain boundary of 0.2C-Nb steel (Buzzichelli and Mascanzoni, 63).
(b) GBD's and IGBD's in an Al bicrystal boundary (Kegg et al, 64).
(c) GBD-macroledges in a grain boundary of Fe-0.75Mn (Ishida et al, 48).
(d) Pure ledges in Fe-0.75Mn (48).

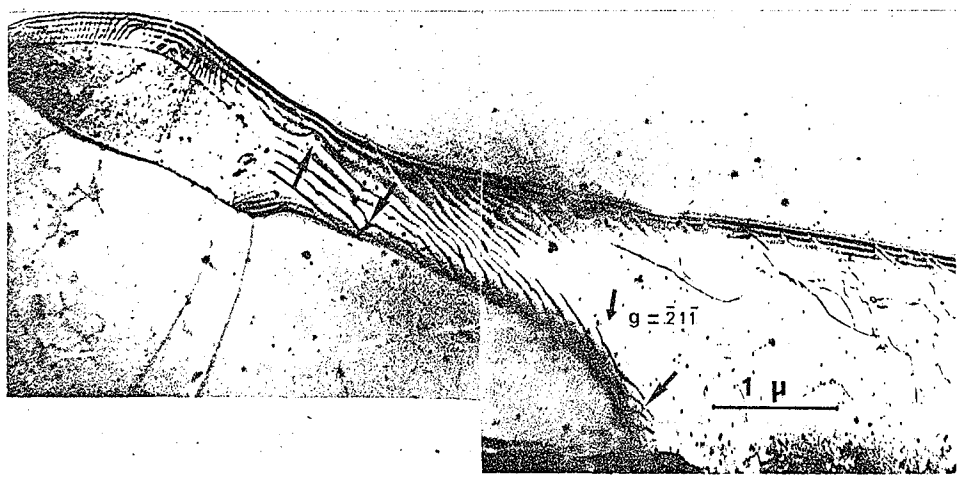

(a)

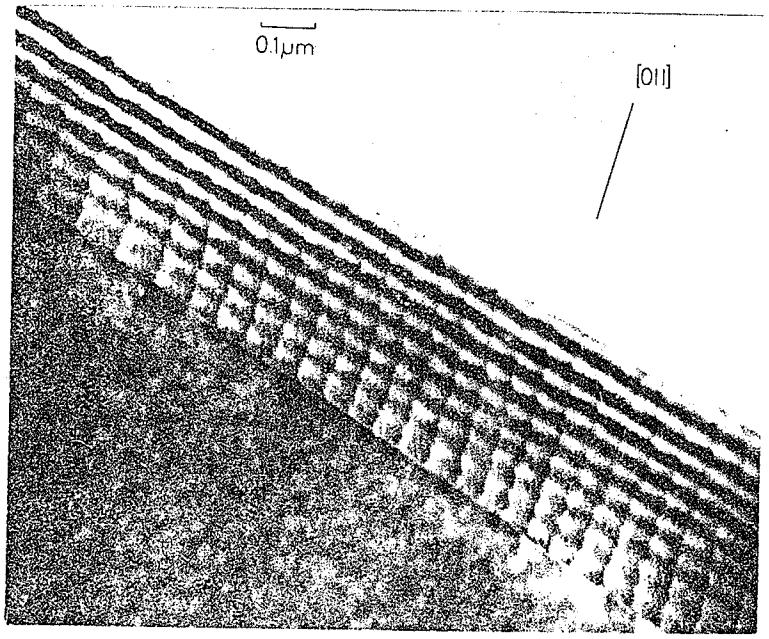

(b)

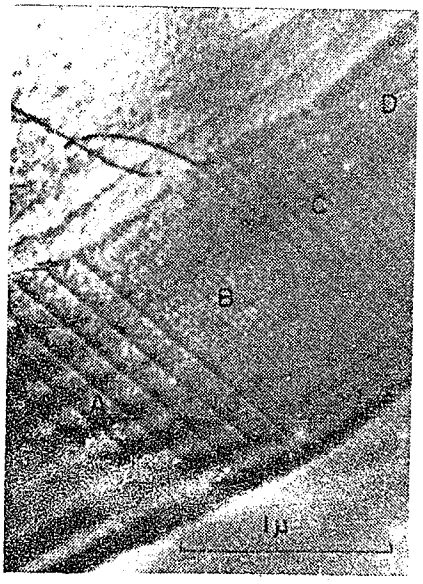

(c)

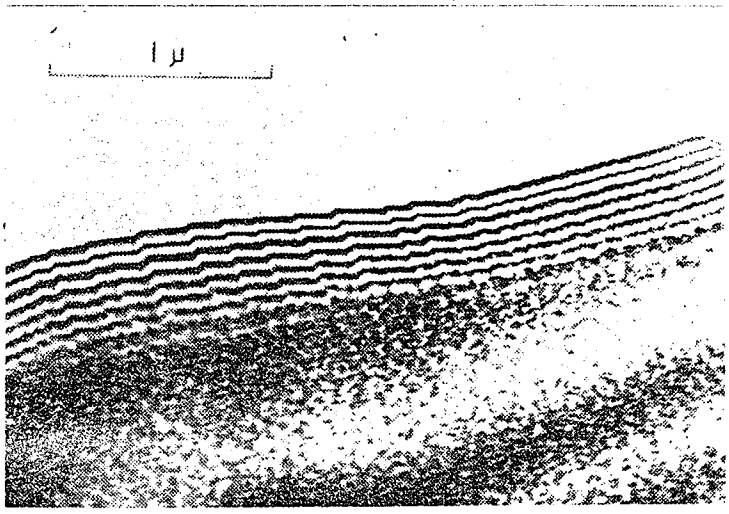

(d)

For figure 17(d), the complete lack of contrast and pronounced fringe shifts easily identify the defects as pure ledges. Unfortunately, cases such as these are the exception rather than the rule and a good deal of thought should generally go into the identification of a boundary defect. For example, the fact that both C-ledges and G-ledges have step characteristics gives rise to the possibility of their creating small fringe displacements (Gleiter has calculated (59) that a 3Å step can, under certain extreme conditions, produce a fringe displacement of over 100 Å). This displacement would be very similar to those from monatomic pure ledges. In addition, the fact that both the C-ledge and the G-ledge have steps of similar dimensions renders them practically identical for pure contrast purposes. We shall later see that this may well have occurred in the literature. A summary of contrast characteristics is given in Table 2.

As with their diffraction contrast, the interactions between boundary defects are being increasingly observed and discussed. Ashby (51) has suggested that supersteps (the equivalent of GBD-macroledges) could form by the combination of several smaller GBD-macroledges, resulting in an energy reduction. In the same way, Ishida and McLean (61) propose that a pure GBD with a Burgers vector

TABLE 2

DIFFRACTION CONTRAST EFFECTS FOR BOUNDARY DEFECTS

DEFECT	CHARACTERISTICS
pure ledge	-small (and occasionally undetectable) to very large boundary fringe displacements -very weak contrast -semi-regular spacing for groups of ledges -generally linear
pure GBD	-no fringe displacement under any conditions -generally strong contrast -generally curvilinear
IGBD	-generally very weak contrast -very small, regular spacing -array covers entire boundary -generally linear
GBD-macroledge	-fringe displacement as pure ledge -contrast as pure GBD -semi-regular spacing for groups -generally linear
C-ledge, G-ledge	-small (and normally undetectable) fringe displacement -varying contrast -generally curvilinear

that is a multiple of the DSC-lattice base vector could be more energetically favorable than a GBD-ledge defect, even though the Burgers vector associated with the latter might be slightly smaller. Both of these thoughts suggest that the majority of GBD-ledge configurations would eventually disappear in a prolonged anneal. There should be no reason why GBD's could not interact with the IGBD network for near-coincidence orientations, as Schober and Balluffi propose (53). However, when the spacing of this network becomes so fine that the IGBD's lose their physical identity, it would seem reasonable to regard any such interaction as unlikely. On the other hand, Pumphrey and Gleiter (65) have observed GBD's "smearing-out" in the boundary plane in the electron microscope and eventually disappearing. One would think that this multiple dissociation would certainly involve the IGBD network. From Pumphrey and Gleiter's observations, it would appear that temperature is the critical factor through its effects on the kinetics of dislocation reactions and possible non-conservative dislocation motion necessary for such reactions. Thus the "smearing-out" phenomenon was a moderately high temperature one.

Finally, Ashby (51) has made some interesting comments on the nature of any boundary dislocations which

stands apart from other boundary defects so as to possess a separate identity. First, outside the dislocation core, they should behave identically to lattice dislocations as far as their long-range elastic strain fields are concerned, i.e. with regard to interactions, line tension, etc. Second, for the core itself, he proposed that it would be elongated in the plane of the boundary and shortened normal to it in order to take advantage of the additional atomic relaxation available therein. As Ashby puts it, this "reflects a balance between the elastic energy stored in the two half-crystals and the misfit or distortion energy associated with the disturbed atom positions in the boundary". He estimated that this would lead to a core energy approximately one-half that of a lattice dislocation, creating, in effect, a binding energy for the GBD to the boundary.

2.4 GRAIN BOUNDARY SEGREGATION

It would be appropriate, at this point, to briefly discuss boundary segregation, i.e. local variation in composition at the boundary, since one solid solution will be studied and even the pure metals to be examined will possess varying numbers of impurity atoms. This will be done with reference to their relation to boundary structure, so that both may later be used to facilitate the understanding

of dislocation generation from boundaries. This area of grain boundary research is somewhat better established than others because of such aspects as grain boundary embrittlement furnishing powerful commercial incentives for its study. In addition, it can be detected, to at least some degree, by relatively simple techniques. Thus several excellent reviews have been written which combine the theoretical models with a substantial amount of experimental data on all aspects of the models. Among these are Gleiter and Chalmer's relatively recent review of equilibrium segregation (21) and Westbrook's reviews on non-equilibrium segregation (66, 67).

2.4.1 EQUILIBRIUM SEGREGATION

At or near grain boundaries, a local variation in composition may exist in equilibrium with the matrix. This is by far the most common segregation encountered, but unfortunately it is rather difficult to quantify or, occasionally, even to detect at all. This may be understood from figure 18(a) which illustrates that the solute concentration at the boundary can be very large, but confined to a region extremely close to the boundary. In the past it has been detected by such means as microhardness, chemical etching, autoradiography and lattice parameter

Figure 18. Schematic representation of the solute profiles at grain boundaries for various bulk solute levels (BSL) for

(a) equilibrium segregation

(b) non-equilibrium segregation due to vacancy migration

(c) non-equilibrium segregation due to boundary migration (boundary movement indicated by arrow).

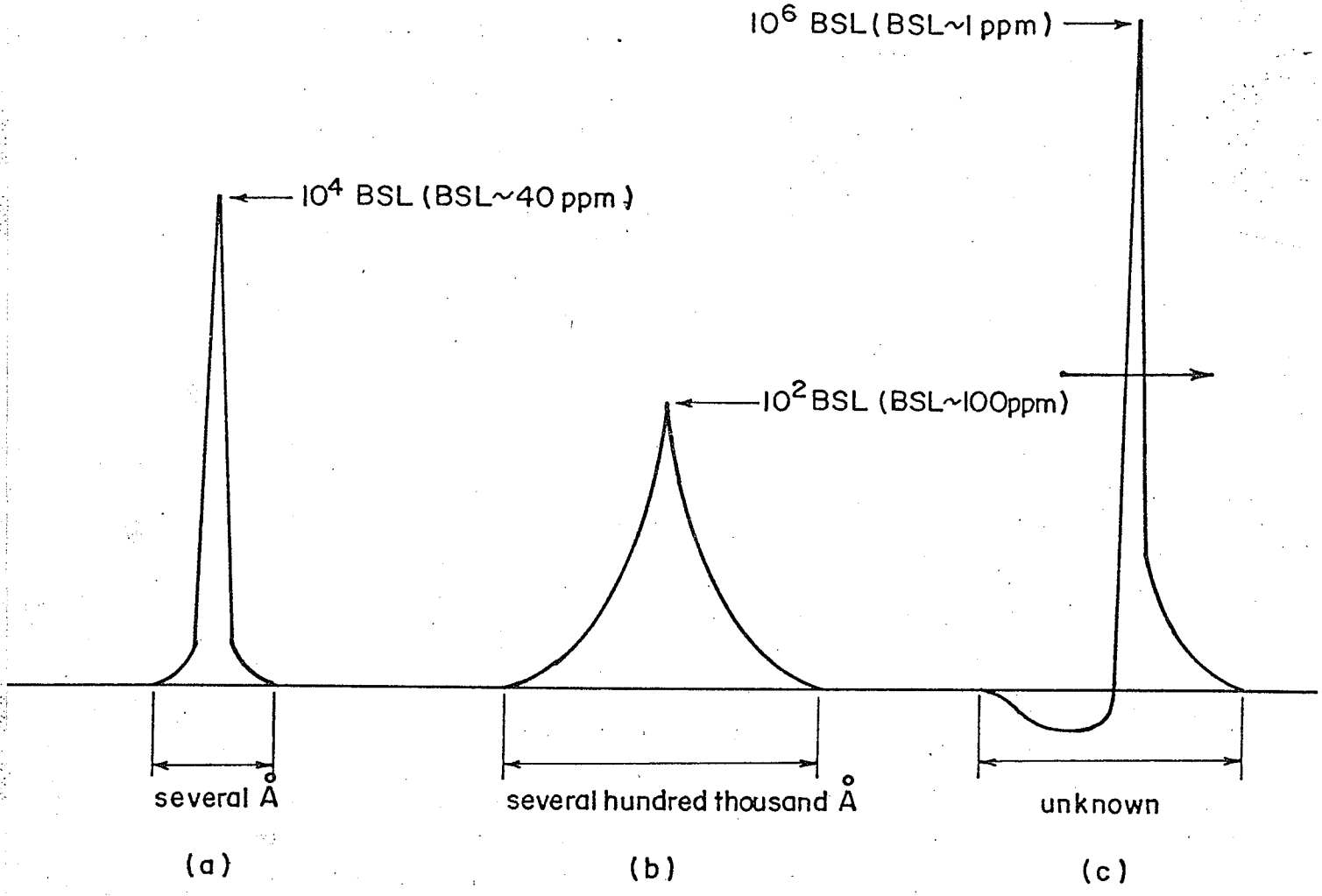
10^6 BSL (BSL~1 ppm)
10^4 BSL (BSL~40 ppm)
10^2 BSL (BSL~100ppm)
several Å
several hundred thousand Å
unknown
(a)
(b)
(c)

variation, but more recent and sophisticated methods such as field ion microscopy and auger electron spectroscopy have been able to quantify it with greater accuracy (21).

The driving force for this segregation may be examined from two different viewpoints. One is that any solute which causes a reduction in the grain boundary energy will tend to segregate to the boundary to lower the energy of the polycrystal as a whole. Such reductions are by no means minor, e.g. Hondros and Seah (68) have shown that as little as 0.5 wt. % Sn reduces the grain boundary energy of Fe by a factor of two.

The second viewpoint, that of elastic interaction, simply states that oversized impurity atoms will migrate to regions of tensile strain (e.g. open spaces) in the grain boundary, while undersized atoms migrate to regions of compressive strain (e.g. overlapping atoms). This approach thus utilizes the structural concept of grain boundaries and the fact that equilibrium segregation of impurity atoms of various sizes exists is verification of the basic physical picture of boundary structure, i.e. a region containing both (+) and (-) strains. Further proof is provided by the fact that non-coincidence (high energy) boundaries show substantially more segregation than coincidence boundaries (21).

In view of the above, it is apparent that, for a given solute, the two critical factors for this segregation are time and temperature, i.e. sufficient time at a high enough temperature will result in an equilibrium amount of the solute being partitioned to the grain boundary. In addition, both theory (21) and experiment (69) show that the equilibrium level increases with decreasing temperature. Thus most quantitative work on this phenomenon involves rapid cooling from the equilibration temperature, because slow cooling would result in levels greater than the equilibrium concentration corresponding to this temperature.

Although equilibrium segregation is normally on a monolayer scale, segregation of a broader nature has been observed in iridium (70) and in Fe - Sn alloys (71) at the higher base solute levels (4 wt. %). In general, the amount of segregation becomes increasingly less sensitive to base solute level at concentrations of these magnitudes. With regard to the degree of enhancement (boundary solute content/bulk solute content), it has been demonstrated both empirically (68) and theoretically (71) that this degree varies as the inverse of the maximum solid solubility of the impurity. Thus, for example, Hondros and Seah (68) obtained enhancements of 3 for Fe-3 wt. % Si (maximum solubility 23 at. %), 460 for Fe-0.2 wt. % Sn (maximum solutility 10 at. %) and 10,000 for Fe-0.0044 at. %S

(maximum solubility 0.1 at. %). This can be useful in predicting the order of enhancement from a given impurity. It is important to note that the effects of multiple impurities are uncertain with regard to any interactions, although Seah and Hondros (71) have found that Sn and S in Fe are non-competitive.

Finally, the pervasiveness of this segregation may be illustrated by the fact that even one part per million (ppm) of certain impurities can, under the right conditions, saturate all the grain boundaries (21). Thus, for all practical purposes, equilibrium segregation is always present to some degree, and its effect on a given property of the grain boundary will depend on the sensitivity of the property to enhanced solute levels.

2.4.2 NON-EQUILIBRIUM SEGREGATION

As implied by the title, these compositional variations are generated by non-equilibrium conditions, such as excess point defect concentrations causing point defect-solute pairs to migrate to the boundaries (which act as sinks for the point defects). Thus, unlike equilibrium segregation, it will ultimately disappear if given enough time. Because of the special driving forces which can cause it, it is much less common than equilibrium

segregation. However, it occurs on a much more detectable scale (figure 18 b), extending as far as 40 microns into the grain interior (72). Thus non-equilibrium segregation is commonly measured by a microhardness increase (up to 35% at the boundary) due to the enhanced solute level. The width of the segregated regions can be so wide that the hardening from opposite boundaries may overlap for smaller grain sizes (72). It should be made clear that the hardness increase due to such segregation is much greater than any microhardness increase attributable to the boundary without solute present, i.e. due to its inherent nature as a highly defected (or strained) region. (The same fact holds for equilibrium segregation). In some cases (73), boundaries also appear to demonstrate a softening effect, likely because of the creation of a vacancy-free zone around them attained when the material is quenched from near the melting point. As with the equilibrium segregation, the enhancement levels are greatest for small amounts of impurities. The illustrative level of figure 18(b) comes from calculations by Anthony (74) based on work in which the base solute level was of the order of 10 - 100 ppm (73, 75).

The most acceptable model of this segregation has been derived primarily by Westbrook and co-workers (73, 75).

It is believed to be caused by the migration of solute - vacancy pairs to the grain boundary during rapid cooling (the effect is markedly reduced by slow cooling (76)). Unlike equilibrium segregation, size misfit does not appear to play the major role, e.g. segregation was found (75) in Zn with Al impurity (atomic radii 1.38 and 1.43 Å, respectively) whereas reverse segregation or boundary softening was found in Pb with Ca impurity (atomic radii 1.75 and 1.97 Å, respectively). It was discovered that the presence of this segregation coincided with a distribution coefficient less than one (ratio of solidus to liquidus concentration at a given temperature), which, in turn, was demonstrated to empirically correlate with a large, positive solute-vacancy binding energy. In addition, it coincided with an activity coefficient (an indicator for the different atomic interactions in a solution) greater than one. This indicates a preference for solute-solute bonds in the system, i.e. good cluster stability. Thus the following picture emerges; a large driving force is obtained upon quenching due to the large number of non-equilibrium vacancies. This, in turn, results in many solute-vacancy pairs (because of the strong binding energy) which migrate towards the most efficient vacancy sinks, the grain boundaries. As these pairs near the

boundary their density increases and collisions take place with increasing frequency, forming di-vacancies and relatively immobile solute clusters. These clusters are thought to give rise to the increased hardness (which, incidentally, is higher than would be expected from the increase of solute in solid solution). Grain boundary softening is also explained by the same model (74, 77) on the basis of the relative mobilities of solute and solvent. Thus, when the solute-vacancy binding energy is of the order of the thermal energy and the solute is quite mobile in the solvent lattice, a net flow of solute away from the boundary can occur because of vacancies using solute atoms as a diffusion path. Since non-equilibrium vacancies are the media for solute transfer, the effect saturates for a solute concentration of a few hundred ppm, which is the order of the maximum non-equilibrium vacancy concentration normally attainable. This also explains the reduction in hardening with a slow cooling rate, since the non-equilibrium vacancy concentration (and, as such, the driving force) is, at a given instant, extremely small. This favors the more mobile single and di-vacancies to migrate to the boundaries instead of the solute-vacancy pairs.

One other theory has been proposed (78), based on the same vacancy-solute mechanism, which predicted maximum

segregation with a slow cooling rate (contrary to the above). This was apparently also confirmed experimentally (79). However, the experimental method used (chemical dissolution of a few microns around the boundary for atomic adsorption spectrophotometry) suffers from the fact that it would have included equilibrium segregation as well, and excluded much of the non-equilibrium segregation. This points out the difficulty in separating the two types of segregation, which, however, must be done in view of the widespread occurrence of equilibrium segregation. A good example of the misinterpretations possible without this dual consideration appears to be provided by a study of binary Cu alloys both quenched and furnace cooled from temperatures ranging from 500 to 1000^{o}C (80). Although the tests were ostensibly a study of equilibrium segregation by means of microhardness tests on the boundary and in the grain interior, the authors stated that "no very great difference" was found in the results for the two cooling rates, contrary to the preceeding discussions for either segregation. Such unexpected results may be explainable via the above dual consideration. Thus, quenching would enhance non-equilibrium segregation, particularly from high temperatures, while slow cooling would enhance equilibrium segregation, particularly from low temperatures, resulting in equivalent

hardness increases even though obtained by different mechanisms. The situation becomes even more complicated when the behaviour of boundary defect densities is also considered. For example, rapid quenching can set up sufficient stresses to cause a very large increase in the density of GBD's and/or GBD-ledges. The multitude of subsequent possible interactions with varying amounts of solute segregation that then arises is very likely the cause of some contradictory stands that have been taken with regard to the influence of these interactions on mechanical behaviour (81, 82).

Mention should be made of one other type of non-equilibrium segregation that applies to super-purity metals and has only recently been detected by Kasen (83). He used high temperature, isochronal anneals to conduct resistivity studies on Al of varying purity (0.5 - 4 ppm). His results indicated that the migrating grain boundaries during the anneals swept up solute as they moved through the lattice. The enhancement that was calculated for this segregation corresponded to equilibrium segregation for a base solute level of 3000 ppm. Since these levels were actually only a few ppm, an additional enhancement above equilibrium levels was obtained (roughly 3000:1). The unusual solute profile associated with such segregation

(figure 18 c) is markedly asymmetrical due to the build-up of solute in front of the moving boundary. It may be pointed out that the profile of figure 18(c) applies at high temperatures, and the room temperature profile will be affected by the cooling rate. Furthermore, the effect practically disappeared at the 4 ppm solute level, thus it should not be significant in metals containing more impurities than this.

In sections 2.2 and 2.3, we have seen that the grain boundary region is far from the simple, unstructured region it was once thought to be. Instead, in most cases, it is a region of both order and disorder, with both its own crystal defects and those from the grain interior present upon it in varying numbers. This variation in the detail of the boundary region may vary, not only from one microstructure to another, but from boundary to boundary within the microstructure, and even from one portion of a boundary to another. Nevertheless, this very complexity can make it possible to postulate <u>detailed</u> interpretations for certain grain boundary phenomena. Such concrete proposals, if proven, will be much more valuable than the general explanations often given, particularly for the role of boundaries in the early stages of yielding.

3 DISLOCATION GENERATION FROM GRAIN BOUNDARIES

Having examined the basic structure of the grain boundary and the crystalline imperfections associated with it, we can now focus our attention on the manner in which this region can produce dislocations at low temperatures and why it does so in preference to the grain interior sources. In view of the relatively recent emergence of this field and the controversies in which it is often embroiled, it would perhaps be appropriate to first examine the previous experimental evidence for such generation.

3.1 EXPERIMENTAL EVIDENCE

As seen in Table 3, the direct visual observation of boundary generation has been quite extensive. The reliability of the evidence was done as objectively as possible, but obviously cannot be considered as final and conclusive. It was felt, though, that this would enable some needed qualitative worth to be placed on the various studies. For example, it was found that numerous cases have occurred in the literature where a reference was made to some other confirmation of boundary generation, even though such generation was only casually mentioned or indirectly inferred. On the other hand, it appears that numerous studies have been conducted in which it was

TABLE 3

EXPERIMENTAL EVIDENCE FOR GENERATION OF DISLOCATIONS FROM GRAIN BOUNDARIES

- all testing at room temperature unless otherwise indicated, all material single phase except where indicated

RELIABILITY A - conclusive proof of generation C - more likely than interior generation
B - high probability of generation D - inconclusive

EP = etch-pitting TEM = transmission electron microscopy

REFERENCE	MATERIAL	EXPERIMENTAL DETAILS	COMMENTS	RELIABILITY
84	Nb	in situ foil heating (TEM)	Very obvious examples of generation.	----
85	Zn	as(84)	Not as obvious as in (84).	----
86	Al	as (84)	No micrographs, but generation mentioned in text.	----
87	18-8 stainless steel	in situ foil straining	Very good pictures of partial and perfect dislocation generation from twin and grain boundaries.	----
88	Fe(99.99)	as (84)	Good sequence of dislocations emanating from supposed Frank-Read source on boundary.	----
89	Al	in situ foil straining (HVEM)	As (86).	----
90	Fe-3Si	20,170 μm gr.diam. near yield point (EP)	Concluded grain interior sources although slip bands against only 1 boundary. Slip initiation stress independent of gr.diam. Higher % of yielded grains in large gr.diam.	B
91	Fe-3Si	30-260 μm gr.diam. near yield point(EP)	Sources generally located on 1 g.b. segment. Most emanation from only 1 side of boundary. Generation into both grains nearly collinear.	A
92	Fe-3Si	90-1600 μm gr.diam. near yield point(EP)	Triple points favored as slip band sites. Interior sources assumed, but slip bands indicated boundary sources, as (90).	A

TABLE 3 (continued)

REFERENCE	MATERIAL	EXPERIMENTAL DETAILS	COMMENTS	RELIABILITY
93	Fe-3Si	premacroyield region (EP)	Enhanced boundary generation in surface grains. Concluded no nucleation involved in boundary generation.	A
94	Fe-3Si	25-800 μm gr.diam. premacroyield region (EP)	Found initiation stress dependant on grain diameter.	B
95	Fe-3Si	10-150 μm gr.diam. (EP)	Only 1 micrograph, which is inconclusive.	D
96	Fe-3Si	1000-5000 μm gr.diam. premacroyield region (EP)	Showed majority of yielded grains to be elastically harder than neighbour grains.	----
97	Fe-3Si	76 μm,pulse loading near yield point(EP)	Conclude boundaries are dislocation sources unless surface scratches are present.	B
98	Fe-3Si	premacroyield region (EP)	Triple points and kinks favored as sources. Higher % of yielded grains in large gr.diam.	A
99	Fe-3Si	(EP)	One micrograph with slip bands emanating from 1 side of 1 boundary.	C
100,101	Fe-3Si	bicrystals near yield point(EP)	Observed primary slip from boundary,interior and crystal surface. Observed secondary slip from boundary.	D
102	β-brass	as (100,101)	Observed secondary slip from boundary.	D
103	Nb(99.85)	30-2300μm gr.diam. near yield point(EP)	Triple points and kinks favored as sources. Observed cases of classical pileup-propagation. Much higher slip band density around boundary than interior at 1.6% strain.	A
104	Cu(99.98)	5000 μm gr.diam.(EP)	Observed primarily interior sources, but some micrographs show slip bands at only 1 boundary.	D
105	MgO	3-100 μm gr.diam. premacroyield region (EP)	Found initiation stress independant of gr. diam. but stress for propagation across grain dependant on same.Observed triple point preferance for slip band location.	A

TABLE 3 (continued)

REFERENCE	MATERIAL	EXPERIMENTAL DETAILS	COMMENTS	RELIABILITY
106	Cu,Ni,Zn Al,Ge	15-110 μm gr.diam. microyield point (slip lines)	Initiation stress dependant on grain diam. Slip began in large grains and spread across grain during premacroyield region.	no figures
107	Pb	bicrystals, 25°-110°C (slip lines)	Observed secondary slip around boundaries, possibly from removal of boundary ledges via dislocation emmission.	C
108	Mg,Al Mg-1Al	large-grained (slip lines)	Observed a zone of secondary slip around the grain boundaries.	C
109	Ti-6Al-4V	quenched from 920°C, aged 4 hr @ 540°C, crept @ 0.9 yield stress for 1000 hr (TEM)	Several figures of likely boundary sources, one clearly showing loops from boundary. Triple points favored. No similar defects seen before straining.	A
110	Ti-5Al-2.5Sn	α-forged,air-cooled from 950°C,3 μm gr. diam.,crept @ 25°C 10,000 hr @ 0.6 yield stress (TEM)	Shows one figure of a grain with clean grain boundaries and extensive dislocation loops bowing out from a triple point.	B
111	Ni-base superalloy	precip.-hardened, crept @ 700°C to 0.2% strain (TEM)	Shows 2 very good micrographs of partial dislocation generation,each of closely adjacent sources. One boundary highly-defected, the other is clean.	A
112	Al	bicrystal (slip lines and TEM)	Concluded sources were in or near the boundary,activated by dislocation pileups.	no figures
113	α-Fe	(TEM)	Shows 1 figure indicating triple point activity. Saw many dislocations near the boundaries.	C
114	Fe(99.6)	55 μm gr.diam., slow-cooled and quenched (TEM)	Observed GBD generation ahead of Luder's front, and some source operation, in slow-cooled material only.	C

TABLE 3 (continued)

REFERENCE	MATERIAL	EXPERIMENTAL DETAILS	COMMENTS	RELIABILITY
115	Armco Fe	(TEM)	Preference for triple points as sources, saw no classical pileups.	B
116	low C steel	strain ageing (EP,TEM)	Observed more boundary sources as fully-aged condition was approached.	EP- B TEM-C
117	austenitic stainless steel	5-10 μm gr.diam., cold-rolled 1-10 % (TEM)	Interior sources assumed, but 1 figure shows bowing away from boundary. Another shows apparent pileups with no matching pileups on opposite boundary. Another shows stacking faults emanating from near a triple point.	B
118	Fe-C	2-phase, cyclic stressing, quenched (TEM)	Boundary generation inferred from precip.-free channels leading into the grain.	D
119	stainless steel	"lightly deformed" (TEM)	Shows 2 figures, each with several adjacent sources of varying clarity.	B
2	304 stainless steel	10-15 μm gr.diam., "lightly cold-rolled" (TEM)	Shows 2 very good figures of dissociated dislocations emanating from boundary ledges. The boundaries are relatively clean.	A
120	as (2)	cold-rolled 1% (TEM)	Shows 2 very good figures with inverse pile-up configurations. Another shows several adjacent sources. Also shows sources in Al.	A
60	as (117)	cold-rolled 2% (TEM)	Shows 1 good figure of what appears to be 2 adjacent sources forming single loops.	A
121	Fe-4P	1000 μm gr.diam. 10 μm subgr.diam. (TEM)	Shows 2 very good figures of dislocation loops emanating from boundaries at 1 and 3% strain.	A
122	Fe-0.9Cu	50μm gr.diam.,0.1% strain (TEM)	Shows 1 good figure of dislocation loops emanating from a boundary.	B
123	Ni_3Fe	ordered (TEM)	Three figures show inverse pileup configurations at boundaries, one at a kink.	B

TABLE 3 (continued)

REFERENCE	MATERIAL	EXPERIMENTAL DETAILS	COMMENTS	RELIABILITY
124	Ni-20Cr	cold-rolled 0.7% (TEM)	One figure shows overlapping stacking faults striking a boundary and causing perfect dislocation emmission into tne next grain. Other boundary sources were observed.	C
39	Ni-11.5Al	(TEM)	One figure shows triple point activity.	C
125	Ni-11.5Al	(TEM)	Several figures of likely boundary sources, one being of either double emission or an interior pileup reflecting off the boundary.	B
126	Ni-11.5Al	(TEM)	Shows 1 good figure of perfect dislocation generation across a grain, causing partial dislocation emission into the next grain.	A
127	43Ni-32Co-25V	ordered, 4% strain (TEM)	Shows 1 good figure of a superdislocation bowing out from a boundary which is covered by κ- phase.	B
128	Cu-23.7Ga	quenched from 780°C (TEM)	Profuse partial dislocation emission from grain boundaries due to transformation stresses.	A
129	Al-38.5Zn	quenched from 435°C (TEM)	Supposed generation from grain boundary particles, but very questionable.	D
130	Cu-10.8Si	(TEM)	Shows formation of κ- phase by partial dislocation emission from both sides of boundaries.	A
131	Be	microstrain region (TEM)	Conclude boundary generation may have taken place.	C
132	Be	as above	As above.	C
133	Nb	(TEM)	Shows 1 good figure of triple point activity.	B
134	Nb	(TEM)	One figure of triple point activity, but some doubt if created by applied stress.	B
135	α-Ti	fine-grained, near yield point (TEM)	One good figure shows dislocations emanating from a boundary, travelling across the grain and causing emission in the next grain. Study found that number of boundary sources increased with increasing boundary area (decreasing grain size).	A

TABLE 3 (continued)

REFERENCE	MATERIAL	EXPERIMENTAL DETAILS	COMMENTS	RELIABILITY
53	Ni(99.6)	40 μm gr.diam.,0.4-12% strain (TEM)	Some figures at lowest strains indicate possible boundary sources, but authors conclude interior sources operate.	C
136	Ni(99.98)	60 μm gr.diam., premacroyield region (TEM)	Observed substantial partial dislocation emission from boundaries at 3×10^{-4} strain, but micrographs not too convincing.	C
54	Ni(99.98)	30-120 μm gr.diam., premacroyield region (TEM)	Observed emission of both perfect and partial dislocations, primarily in the smallest grain size material. One very good micrograph shows 3 adjacent sources emitting loops into the grain interior. Boundary sources were much less in evidence around the macroyield point.	A

tacitly or expressly assumed that any dislocations or dislocation pile-ups associated with the boundary had originated at grain interior sources. This was often done even though the visual evidence suggested otherwise, likely because of the relatively new nature of the idea of boundaries acting as sources. In still other studies, pictorial evidence of likely boundary generation is incidental to the main purpose of the study and is not commented on at all. In compiling Table 3, an attempt was made to indicate such circumstances where possible. Several examples of boundary generation are shown in figure 19.

Leaving the implications to be discussed later, some of the points that can be extracted from Table 3 are:

1. The studies conducted inside the electron microscope have conclusively shown that both grain and twin boundaries are the major dislocation sources in thin foils. At the same time, extensive GBD movement can take place in the boundaries of such foils.
2. Boundary generation has been quantitatively documented in only one material, Fe-3Si, but the qualitative evidence for other materials shows that a wide range of metals and alloys possessing the three major crystal structures (BCC, FCC, HCP) are capable of boundary

Figure 19. Examples of dislocation generation from grain boundaries in

(a) Ti-6Al-4V (Odegard and Thompson, 109)

(b),(c) Fe-3Si (Tandon, 137)

(d) austenitic stainless steel (McDonald and Ardell,60).

(e) 304 stainless steel (Murr, 120)

(f) Ni (Malis et al, 54)

(g) Ni-11.5Al (Baro and Hornbogen, 126).

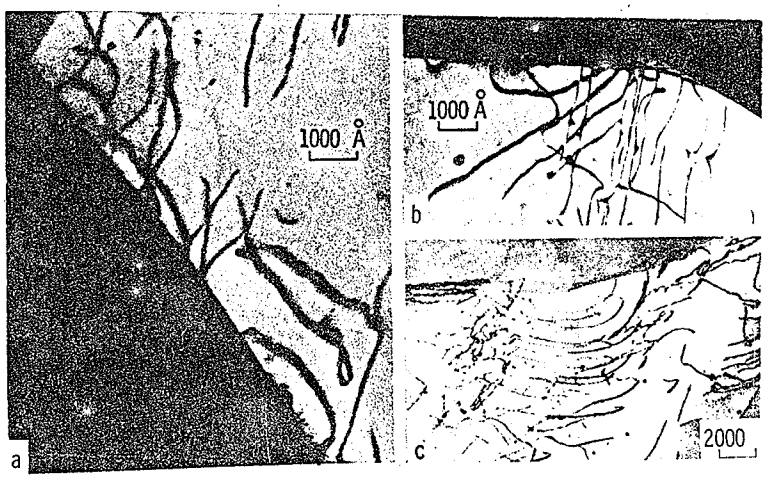

(a)

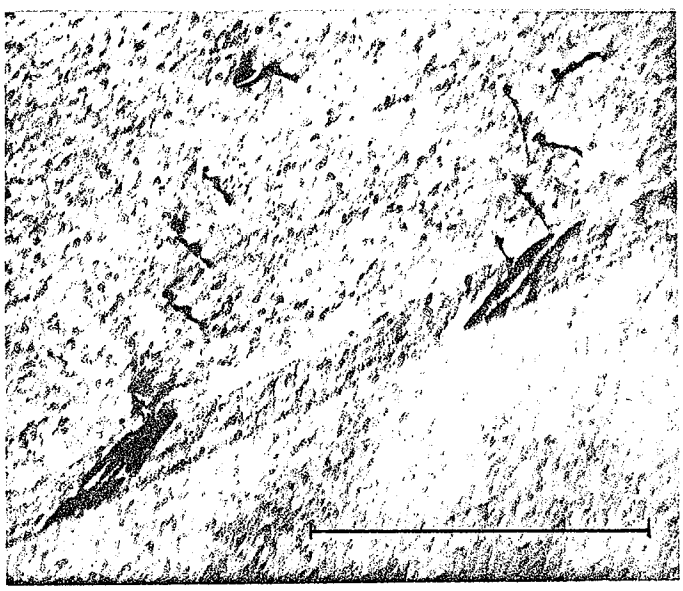

(b)

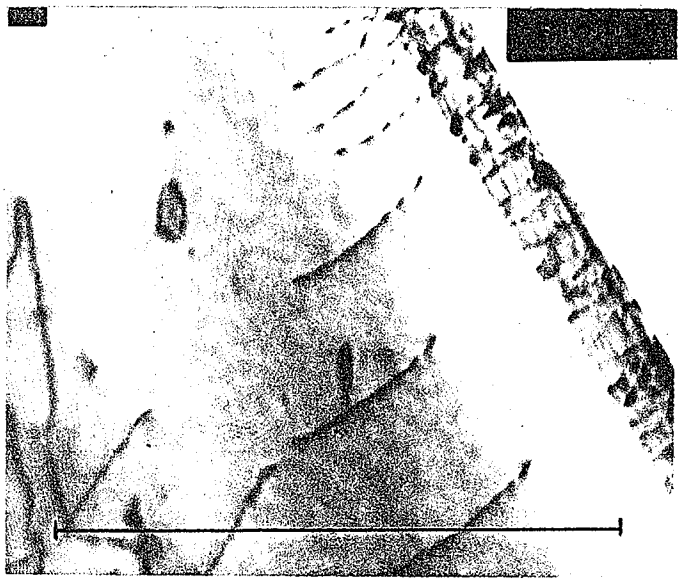

(c)

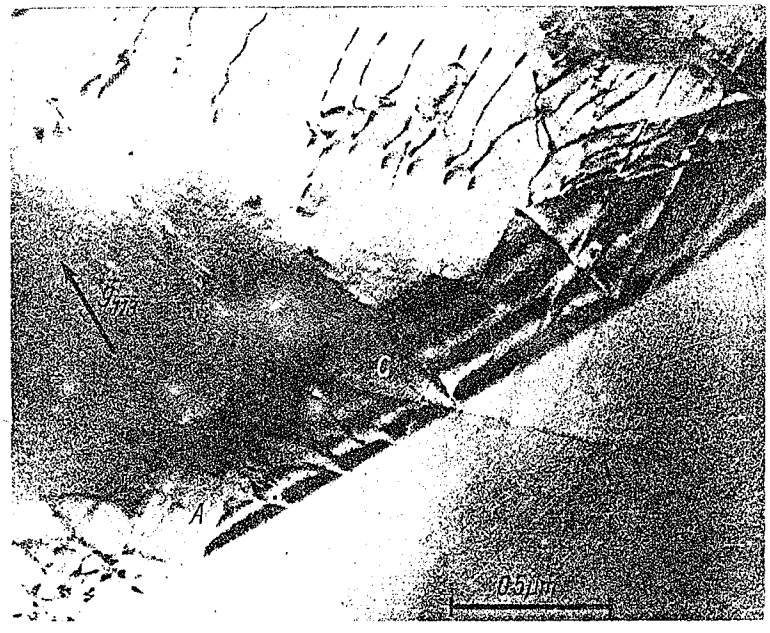

(d)

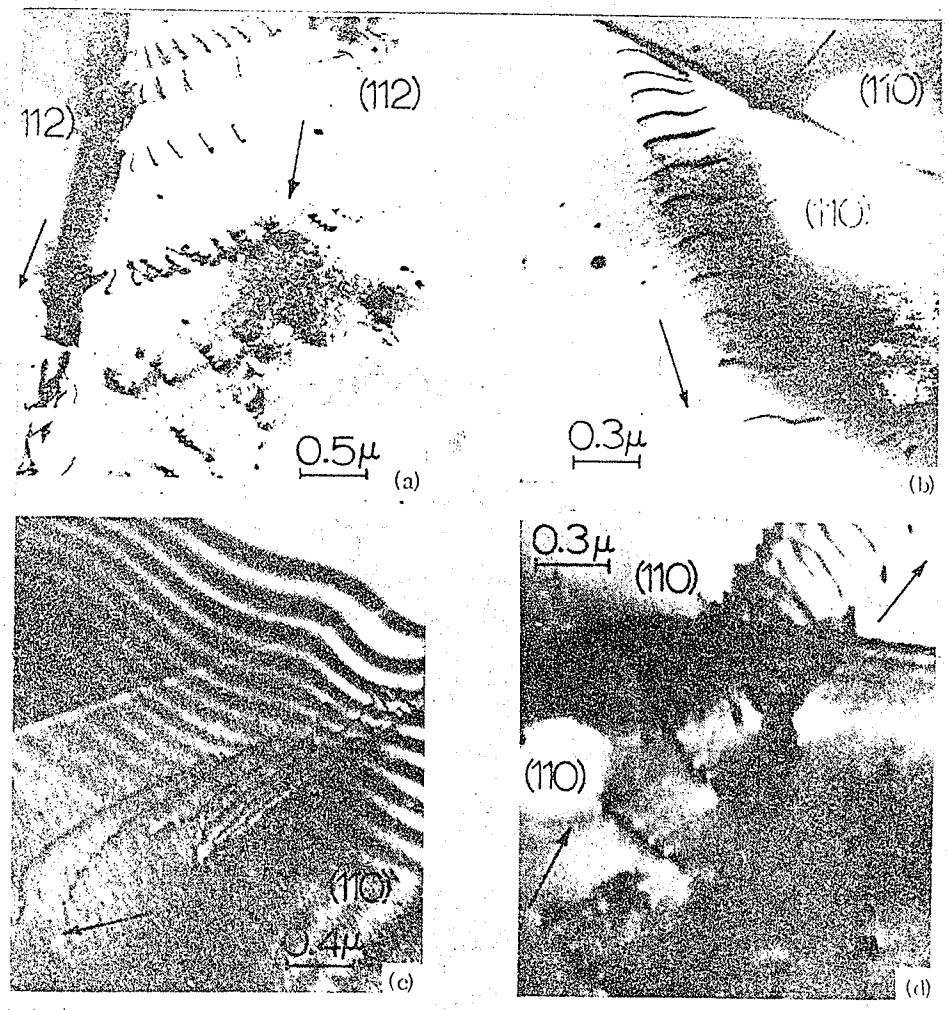

(e)

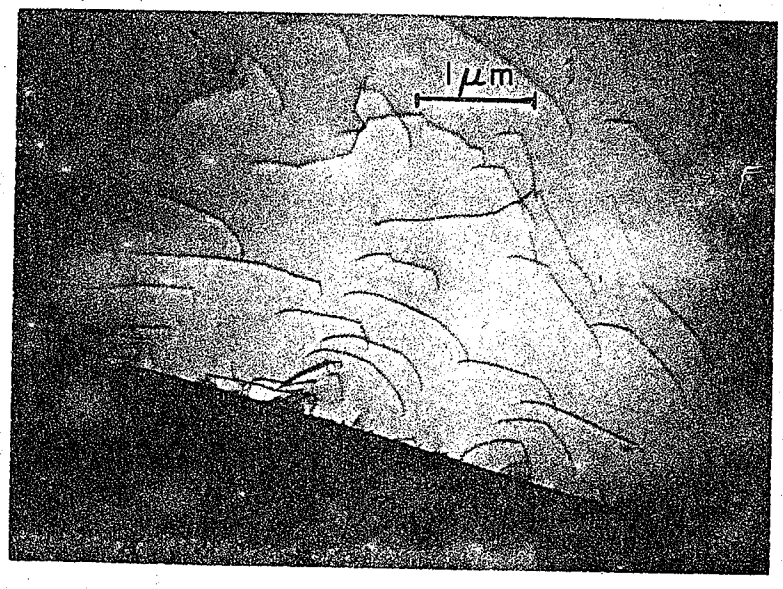

(f)

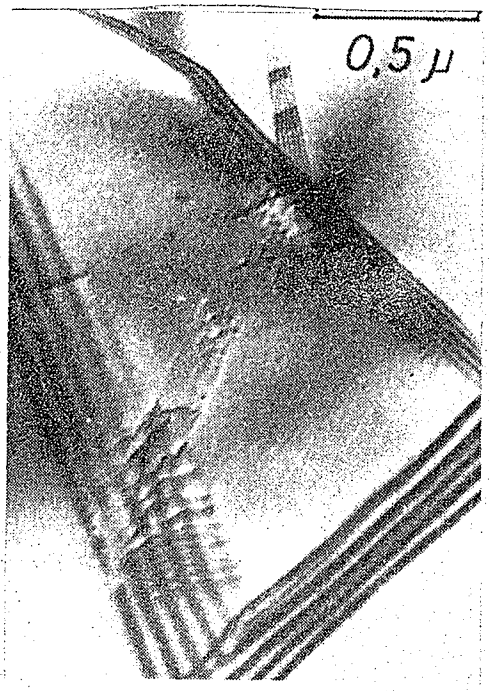

(g)

generation. Some of these have been indicated by both etch-pitting and electron microscopy, e.g. Nb (103, 134) and low carbon steel (116).

3. Boundary generation occurs preferentially at triple points (39, 42, 92, 98, 103, 105, 115, 117, 123, 133).
4. Generation occurs normally from only one boundary of a grain and from one side of that boundary (91, 105).
5. When generation does take place into both grains, it is collinear (or nearly so) (91, 105).
6. There is a higher percentage of yielded grains in large-grained material (90, 98).
7. Generation from boundaries appears to occur more readily in fine-grained material, e.g. less than 100 μm grain diameter, especially for pure metals (2, 105, 106, 110, 114, 117, 122, 135, 53, 136, 42).
8. Interior sources occur more and more frequently as grain diameter increases (103, 104).
9. Boundary sources in surface grains appear to operate at stresses slightly lower than those in interior grains (93).
10. There is some doubt as to whether the source operation stress is dependent on grain diameter (93, 106) or independent of it (90, 105).
11. Generation appears to occur preferentially in grains

of high elastic modulus (96).

12. Boundary generation can be caused or enhanced by elastic and plastic incompatibility and elastic anisotropy (100 - 102, 107, 108).
13. The classical theory of yield propogation across a grain boundary by means of dislocation pile-ups against it has been observed in conjunction with boundary generation (100, 101, 103, 112, 124, 126, 135).
14. Generation of partial dislocations can occur in metals of both low and high stacking fault energy (117, 2, 124, 126, 128, 130, 42).
15. Although the majority of evidence for dislocation generation from grain boundaries has been observed at or below the macroyield stress, a number of studies indicate that it can also occur at higher strains (117, 120, 60, 121, 127).

It is unfortunate that the bulk of the more quantitative data has been confined to only one material, Fe-3Si, and has been derived by only one experimental technique, etch-pitting. The difficulties of obtaining reliable quantitative data from electron microscopy of boundary generation will be discussed later, but suffice it to say at this point that they are both numerous and severe. It should be noted that some preliminary electron

microscopy of Fe-3Si in this laboratory does appear to confirm boundary generation in that material (137). Finally, it should be mentioned that several studies have hypothesized that boundaries could act as dislocation sources, in order to explain other experimental results (86, 134, 138-143).

3.2 GRAIN BOUNDARY DISLOCATION GENERATION MODELS

From the first detection of boundary dislocation generation, models of varying degrees of complexity have been proposed to explain how the generation process occurs. These models have been categorized by Tangri et al (179) as those which require low temperature GBD glide to activate the source, and those which may require GBD glide only to keep the source active. In other words, in the first category GBD glide is necessary before the source operation, while in the second it may only be necessary during the operation. This glide is over relatively short distances in the boundary and thus should not be confused with the proposed large scale gliding (sliding) that Gifkins and Langdon (108) have shown to be erroneous.

3.2.1 MODELS NOT REQUIRING GBD GLIDE

The earliest, and most well-known of these models is that of Li (144) and it is exceedingly simple. A grain

boundary ledge may be viewed as an adsorbed edge dislocation (figure 20a) which, under an appropriate stress, τ, may be expelled into the lattice (figure 20b). One characteristic of this model is the fact that a residual GBD will be left at the boundary if the Burgers vector of the GBD at the ledge is not that of a lattice dislocation. It is important to note that the ledge involved is actually the C-ledge defect discussed earlier, a defect which, unlike pure ledges, does not necessarily have to be present in the grain boundary. This is a major weak point in Li's theory that yielding could take place by emission of dislocations from all ledges to form a network near the boundary which would control subsequent dislocation movement. Also, the ledge itself must be oriented so that it lies along the intersection of a slip plane and the boundary plane, but Price and Hirth (145) mention that this is generally the case. The dislocations produced from such sources would be pure edge and, most important, the sources would be non-regenerative, that is only one dislocation would be produced from each one.

A similar use of C-ledges has been incorporated into two more complex models by Orlov (146), one regenerative and the other not. The non-regenerative model (figure 21a), denoted the Orlov I model, uses the two ledges (A and B) of a boundary facet which can travel into the crystal as

Figure 20. (a) A grain boundary ledge viewed as equivalent to the extra half-plane of an edge dislocation. (b) Annihilation of the ledge by emission of an edge dislocation into the grain interior (Li,144).

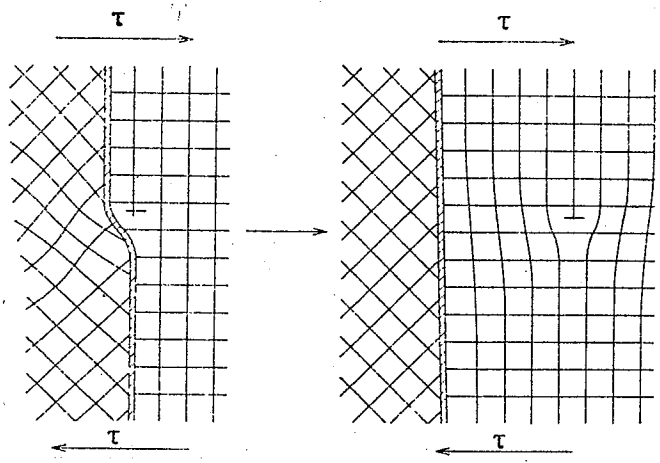
τ
τ
τ
τ
(a)
(b)

Figure 21. (a) Grain boundary facet AB on the surface of a crystal oriented so as to posess two primary slip planes, I and II.

(b) Annihilation of the facet by means of the two ledges travelling into the crystal as edge dislocations on the two slip planes.

(c) Formation of a new facet A'B' on the opposite surface of the crystal (Orlov, 146).

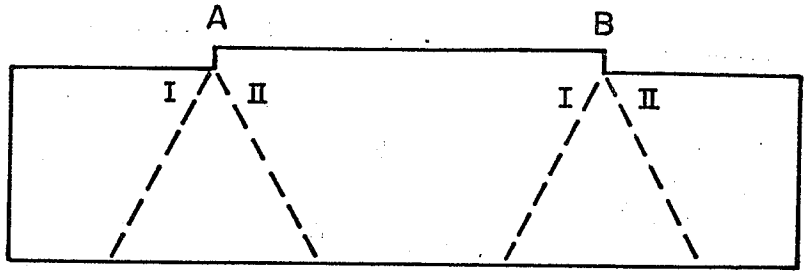

(a)

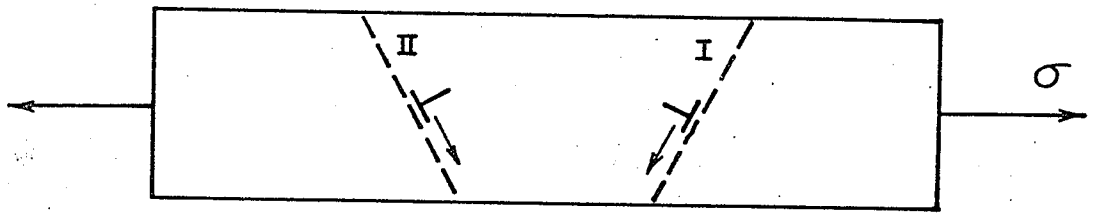

(b)

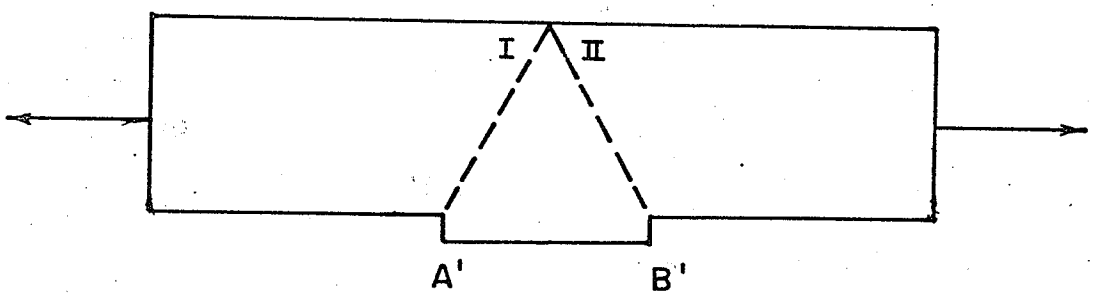

(c)

edge dislocations on either of two equally - likely slip systems (I and II). Under an applied stress, σ, the dislocations travel into the grain on both planes, as shown in figure 21(b). Traversing the grain, they form similar ledges on the opposite grain boundary (figure 21c). In a continued response to the stress, these ledges also emit edge dislocations, but on the opposite slip plane to that used to create the ledge. Again, these emerge on the top boundary and the process continues until the facet disappears (A compressive stress would have the opposite effect and the facet would grow until stopped by some obstacle). In essence, then, plastic deformation occurs through the repeated operation of single dislocation sources and the long range movement of the generated dislocations.

The regenerative model (Orlov II) is even more complex. Starting again with the facet AB and two equally-likely slip systems (figure 22a), we can see that the B ledge (abcd) travels into the grain as a dislocation loop (efgh) on plane I (figure 22b). This loop annhilates the original ledge and creates two new ledges, (cei) and (dbh). Since these are A-type ledges, they can travel into the grain as dislocation loops (ejkl) and (mnop) on plane II (figure 22c). The segments (kl) and (mn) of these loops recreate a B-type ledge (cqrd) as they meet

Figure 22. (a) Grain boundary facet AB with slip planes I and II.
(b) Removal of ledge B by emission of an edge dislocation on plane I.
(c) Re-creation of the ledge B by emission of edge dislocations on plane II (Orlov, 146).

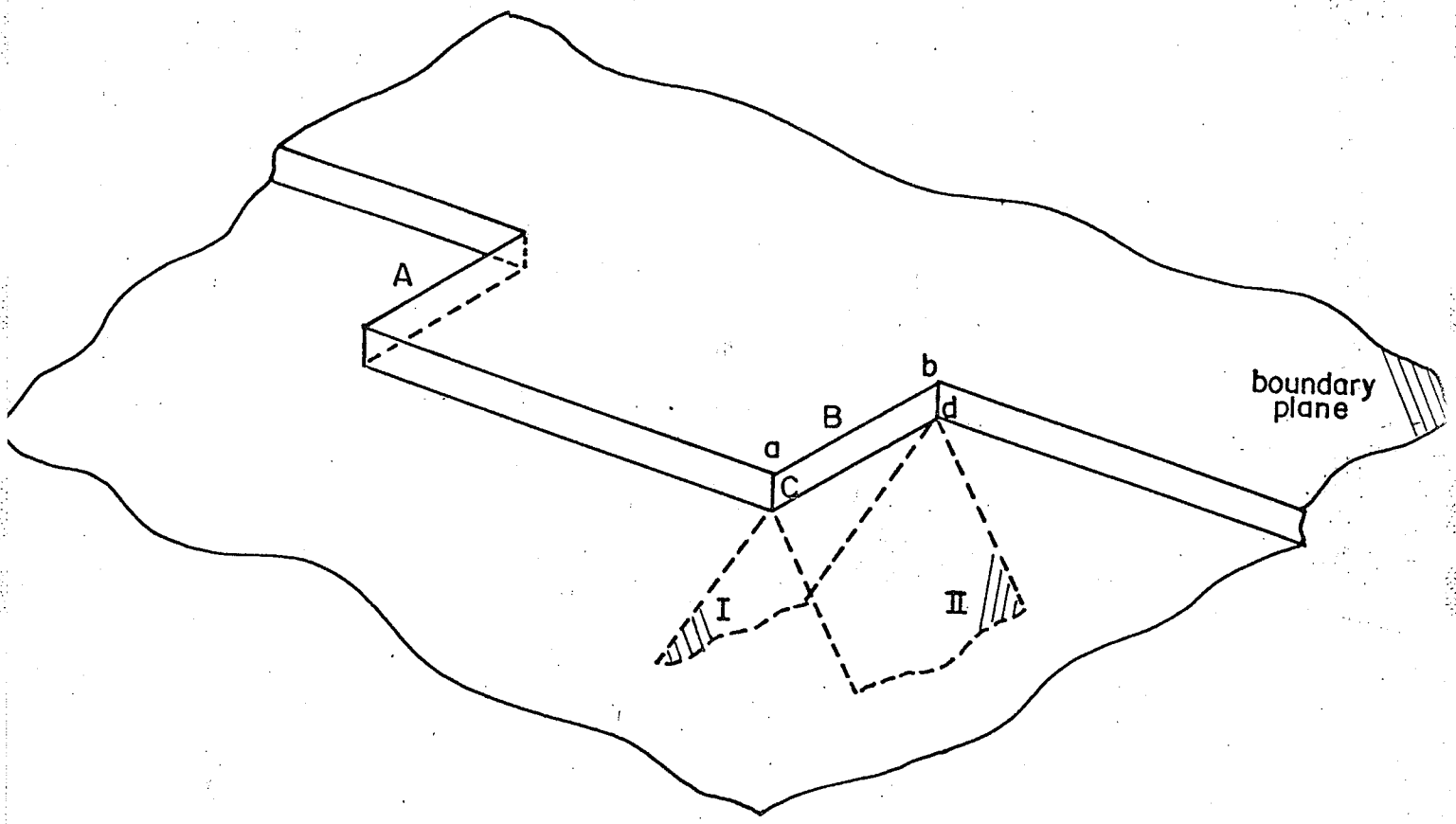
A
B
C
a
b
d
boundary plane
I
II

(a)

(b)

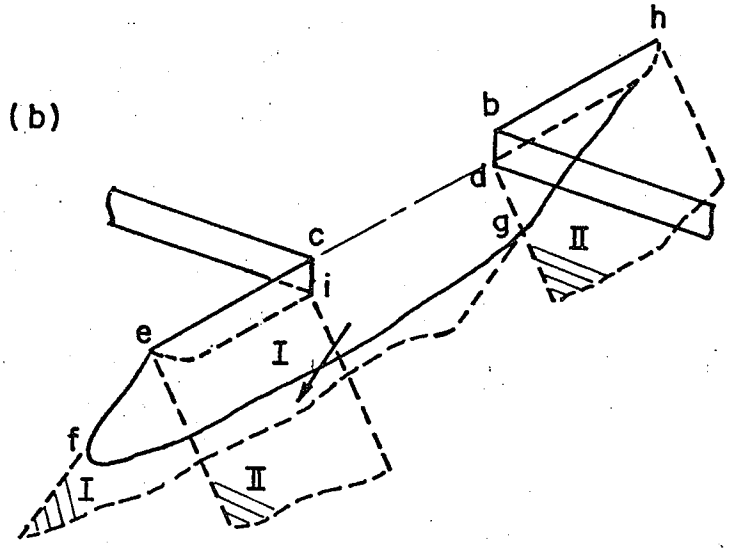
h
b
d
c
g
II
i
e
I
f
I
II

(c)

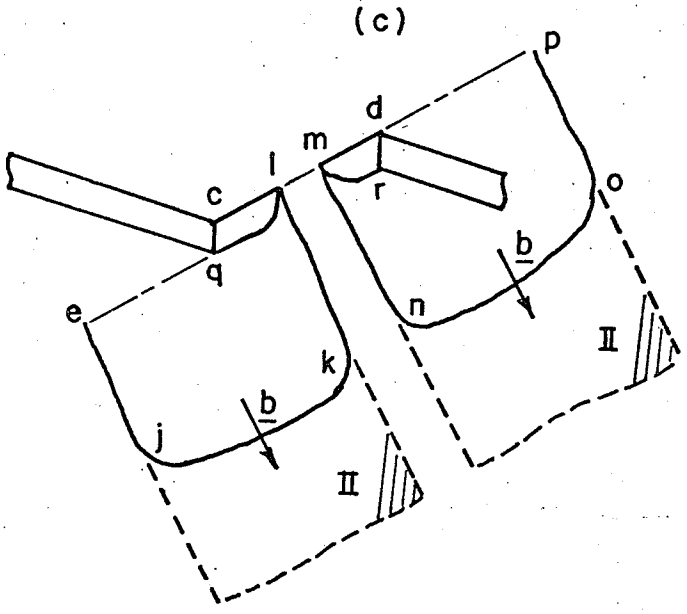
p
d
m
l
c
r
o
b
q
e
n
II
k
b
j
II

and annhilate each other. The entire process then begins anew. Since a similar process is occurring at A, the end result is four adjacent dislocation sources. It is also interesting to note that the process essentially results in grain boundary migration, i.e. the upper grain has grown at the expense of the lower one in figure 22.

Given the large number of grains in a polycrystal, it would seem reasonable to expect that some small percentage would be oriented so as to possess two equal slip systems. Other difficulties do arise, however. The first model requires that the free slip length of both dislocations be the same. Similarly, in the second model, any obstacle which stops any one of the four dislocation "trains" should hinder or even stop the operation of the entire process. For small facets this could quite easily be the interaction of the dislocations from each ledge. A similar cessation could occur if cross-slip and tangling occurred. As in the Li model, residual GBD's would be left at the boundary, since the ledge could only be oriented on one of the two slip planes. The accumulation of these would also hinder the source since they would not necessarily be glissile in the plane of the boundary. As before, the ledges would have to lie along the intersection of the slip plane and boundary.

Another model incorporating two slip planes has been suggested by Gleiter et al (125). In this model (Gleiter I), it was proposed that generation of an equal number of screw dislocations on each slip plane (figure 23) would enable continuity to be maintained at the boundary. No mention was made, however, of the details of this process.

A similar, more detailed model has since been proposed by Price and Hirth (145), although generation on only 1 plane is necessary. As shown in figure 24, the model simply proposes that, for every amount $\overline{b}$ (Burgers vector) the screw ledge shears, one screw lattice dislocation is emitted. Continuity at the boundary is maintained by the simultaneous creation of compensating GBD's which are glissile in the boundary (figure 25). The authors note that the generated loops will eventually intersect other portions of the boundary, creating ledges which will act as a drag on the continued propogation of the loop. If the character of the ledge is mixed, its area will decrease as the edge component vanishes due to Li-type behaviour. Although there seems no reason why pure ledges could not act as sources, the authors conclude that the GBD-macroledge defect would be more likely since it possesses a higher energy.

Figure 23. (a) Grain boundary with slip planes ABCD and ABEF intersecting along <110> at the boundary.
(b) Generation of screw lattice dislocations in equal numbers on both planes (Gleiter, 125).

Figure 24. Generation of a screw lattice dislocation from a grain boundary ledge by shear of the ledge by one Burgers vector (Price and Hirth, 145).